NIKHEF/96-018
ITP-SB-96-16
INLO-PUB-08/96

$O(\alpha_s^2)$ corrections to polarized heavy flavour production at $Q^2 \gg m^2$

M. Buza [1]
NIKHEF/UVA,
POB 41882, NL-1009 DB Amsterdam,
The Netherlands.

Y. Matiounine and J. Smith [2]
Institute for Theoretical Physics,
State University of New York at Stony Brook,
New York 11794-3840, USA.

W.L. van Neerven
Instituut-Lorentz,
University of Leiden,
PO Box 9506, 2300 RA Leiden,
The Netherlands.

August 1996

Abstract

In this paper we present the analytic form of the heavy flavour coefficient functions for polarized deep inelastic lepton-hadron scattering. The expressions are valid in the kinematical regime $Q^2 \gg m^2$ where Q^2 and m^2 stand for the masses squared of the virtual photon and heavy quark respectively. Using these coefficient functions we have computed the next-to-leading order α_s corrections to polarized charm production at HERA collider energies, where both the electron and proton beams are polarized. We also give an estimate of these corrections at fixed target experiments where the typical Q^2 values are much smaller than at HERA.

[1]supported by the Foundation for Fundamental Research on Matter (FOM)
[2]partially supported under the contract NSF 93-09888

1 Introduction

Apart from another test of perturbative QCD, deep inelastic electroproduction of charm quarks leads to important information about the gluon density inside the proton [1], [2], [3], [4]. This is because the dominant production mechanism is represented by the (virtual) photon-gluon fusion process [5] which is the only one appearing in the Born approximation. Although in higher order of the strong coupling constant α_s other subprocesses will also contribute it turns out that the above picture remains essentially unaltered.

Until now almost all attention was paid to unpolarized charm production. However in future fixed target [6] as well as collider [7], [8] experiments one is also interested in charm production in polarized deep inelastic lepton-hadron scattering (the case of photoproduction has recently been discussed in [9] and [10]). Like in the unpolarized case one is particularly interested in the gluon density since it plays an important role in the description of the longitudinal spin structure function $g_1(x, Q^2)$. Here x denotes the Bjorken scaling variable and Q^2 is the mass squared of the virtual photon exchanged between the lepton and the hadron. Contrary to unpolarized charm electroproduction, where the cross-section is already calculated up to next-to-leading order (NLO), only the Born approximation exists for the polarized case [11], [12], [13]. The calculation of the NLO corrections will be as difficult as that for unpolarized charm electroproduction in [14], which could be only done in a semi-analytic way. This is because the cross sections for the parton subprocesses involve four dimensional phase space integrals where the integrations over the azimuthal and polar angles can be performed analytically. The two remaining integrations have to be done numerically. After mass factorization the resulting coefficient functions are folded with parton densities so that one finally has to do integrations over three variables. Furthermore the LO parton cross sections for F_L and F_2 in the unpolarized case are positive definite in contrast to those for the spin structure function g_1. After mass factorization the positive definiteness does not apply to the NLO coefficient functions in F_L and F_2 anymore and additional positive and negative parts appear for those in g_1. This leads to large cancellations in the numerical integrations which will particularly complicate the computation of g_1. Hence the semi-analytic calculation of g_1 will be harder than that already carried out for F_L and F_2 in [14]. Therefore it is important to have an analytic form of the heavy quark coefficient functions in some kinematical regime that can

serve as a check on the exact $O(\alpha_s^2)$ calculations which have still to be done for the spin structure function g_1. Fortunately, as has been shown for F_L and F_2 in [15], one can obtain analytic expressions for the heavy quark coefficient functions in the asymptotic region $Q^2 \gg m^2$. Here the asymptotic formulae for the heavy quark coefficient functions could be inferred from the operator matrix elements (OME's) and the light parton coefficient functions so that one did not have to resort to cumbersome calculations of loop- and phase-space integrals.
As far as phenomenological applications are concerned, the asymptotic heavy quark coefficient functions will be a good approximation at HERA collider energies, where both the electron and the proton beams are polarized, because there will be events at $Q^2 \gg m_c^2$, where m_c is the mass of the charm quark. At fixed target energies, where Q^2 is small, this approximation will break down but one can partially remedy this by also including threshold effects which are due to soft gluon bremsstrahlung. The latter mechanism dominates the threshold region of heavy flavour production as is e.g. shown in [16], [17] for hadron-hadron scattering. By including these threshold effects one can obtain a reasonable description of the charm production cross section at small Q^2. We can show this for the unpolarized case since here the exact coefficient functions are available [14], [18]. Due to the similarity between the polarized and the unpolarized cross sections in the threshold region one can assume that this approximation will also work for $g_1(x, Q^2, m^2)$. In this way one can estimate the NLO effects at the much smaller Q^2 values characteristic of fixed target experiments.

The content of the paper can be summarized as follows: in section 2 we introduce our notations and give, for polarized Compton scattering, an exact analytic expression for the heavy quark coefficient function, which is valid for any Q^2 and m^2. In section 3 we compute the full two-loop spin dependent operator matrix elements (OME's) contributing to the spin structure function $g_1(x, Q^2)$. The spin dependent heavy quark coefficient functions will be presented in section 4 in the limit $Q^2 \gg m^2$. In section 5 we give improved expressions for them by including threshold contributions so that they can be also used at smaller Q^2 values. Furthermore we make estimates of the NLO corrections to polarized charm production at HERA collider as well as fixed target energies. The long formulae obtained for the full operator matrix elements and the asymptotic heavy quark coefficient functions are presented in appendices A and B respectively.

2 Heavy flavour production in polarized electron-proton scattering

In this section we present the formulae needed to describe polarized heavy flavour electroproduction. Furthermore we summarize the findings in [15] how to derive the asymptotic form of the heavy quark coefficient functions from the operator matrix elements and the light parton coefficient functions. Heavy flavour production in polarized deep inelastic electron-proton scattering proceeds via the following reaction

$$e^-(\ell_1) + P(p) \to e^-(\ell_2) + Q(p_1)(\ \overline{Q}(p_2)\ ) + {}'X'\,. \tag{2.1}$$

Here $'X'$ represents any final inclusive hadronic state and the momenta of the heavy quark (anti-quark), denoted by $Q(\bar{Q})$, are given by p_1 and p_2 respectively. The mass of the heavy quark $Q(\bar{Q})$ is given by m. Neglecting electro-weak radiative corrections the above process is dominated by the exchange of one vector boson which carries the momentum $q = \ell_1 - \ell_2$.
If the virtuality of the exchanged vector boson $Q^2 = -q^2 > 0$ is not too large ($Q^2 \ll M_Z^2$) reaction (2.1) proceeds via the exchange of one photon only. In this case the computation of the cross-section of (2.1) involves the hadronic tensor

$$W_{\mu\nu}(p,q,s) = \frac{1}{4\pi}\int d^4z\, e^{iq\cdot z} < p,s|[J_\mu(z), J_\nu(0)]|p,s >\,, \tag{2.2}$$

where J_μ stands for the electro-magnetic current and s denotes the spin vector of the proton with $s^2 = -1$ and $s.p = 0$. The hadronic structure tensor can be split into symmetric and antisymmetric parts in the following way

$$W_{\mu\nu}(p,q,s) = W^S_{\mu\nu}(p,q) + W^A_{\mu\nu}(p,q,s)\,, \tag{2.3}$$

$$W^S_{\mu\nu}(p,q) = \frac{1}{2x}\Big(g_{\mu\nu} - \frac{q_\mu q_\nu}{q^2}\Big)F_L(x,Q^2) + \Big(p_\mu p_\nu - \frac{p.q}{q^2}(p_\mu q_\nu + p_\nu q_\mu) + g_{\mu\nu}\frac{(p.q)^2}{q^2}\Big)\frac{F_2(x,Q^2)}{p.q}\,, \tag{2.4}$$

$$W^A_{\mu\nu}(p,q,s) = -\frac{M}{2p.q}\epsilon_{\mu\nu\alpha\beta}q^\alpha[s^\beta g_1(x,Q^2) + (s^\beta - \frac{s.q}{p.q}p^\beta)g_2(x,Q^2)]\,, \tag{2.5}$$

where M is the mass of the proton and x stands for the Bjorken scaling variable (see below). The structure functions F_L and F_2 already show up in unpolarized electron-proton scattering and the heavy flavour contributions have been extensively discussed up to next-to-leading order (NLO) in the strong coupling constant α_s in [14]. If the incoming electron and proton are polarized then in addition to F_L and F_2 one also gets the longitudinal spin structure function g_1 and the transverse spin structure function g_2. The latter show up in the polarized electron-proton cross-section

$$\frac{d^3\sigma^{\overrightarrow{\rightarrow}}}{dxdyd\phi} - \frac{d^3\sigma^{\overleftarrow{\rightarrow}}}{dxdyd\phi} = \frac{4\alpha^2}{Q^2}\Big[\Big\{2 - y - \frac{2M^2x^2y^2}{Q^2}\Big\}g_1(x,Q^2) - \frac{4M^2x^2y^2}{Q^2}g_2(x,Q^2)\Big]\,, \tag{2.6}$$

$$\frac{d^3\sigma^{\overset{\uparrow}{\rightarrow}}}{dxdyd\phi} - \frac{d^3\sigma^{\overset{\downarrow}{\rightarrow}}}{dxdyd\phi} = -\frac{4\alpha^2}{Q^2}\cos\phi\Big(\frac{4M^2x^2}{Q^2}\Big)^{1/2}\Big(1 - y - \frac{M^2x^2y^2}{Q^2}\Big)^{1/2} \times[yg_1(x,Q^2) + 2g_2(x,Q^2)]\,. \tag{2.7}$$

The scaling variables x and y are defined by

$$x = \frac{Q^2}{2p.q}\,, \quad (0 < x < 1)\,. \qquad y = \frac{p.q}{p.\ell_1}\,, \quad (0 < y < 1)\,. \tag{2.8}$$

The angle between the spin $\vec{s}$ of the proton and the momentum $\vec{\ell}_2$ of the outgoing electron in (2.1) is denoted by ϕ. The lower arrows on σ in (2.6), (2.7) indicate the polarization of the incoming electron in the direction of its momentum $\vec{\ell}_1$. The upper arrow on σ in (2.6) stands for the polarization of the proton which is parallel or anti-parallel to the polarization of the incoming lepton. The vertical arrows in (2.7) also belong to the proton which is now polarized perpendicular (transverse) to the polarization of the lepton in either the up or the down direction. In the subsequent part of this paper we will limit ourselves to $g_1(x,Q^2)$ since it contains leading twist two operators only whereas $g_2(x,Q^2)$ can also receive twist three contributions. In the case of twist two the structure functions can be described by the QCD-improved parton model. In this model the heavy flavour contribution to g_1 can be expressed as convolution integrals over the partonic scaling variable

$z = Q^2/(s+Q^2)$ where s is the square of the photon-parton centre-of-mass energy ($s \geq 4m^2$). This yields the following result

$$\begin{aligned} g_1(x,Q^2,m^2) = \frac{1}{2}\int_x^{z_{\max}} \frac{dz}{z}\Big[\frac{1}{n_f}\sum_{k=1}^{n_f} e_k^2\Big\{\Sigma\Big(\frac{x}{z},\mu^2\Big)L_q^{\rm S}\Big(z,\frac{Q^2}{m^2},\frac{m^2}{\mu^2}\Big) \\ +G\Big(\frac{x}{z},\mu^2\Big)L_g^{\rm S}\Big(z,\frac{Q^2}{m^2},\frac{m^2}{\mu^2}\Big)\Big\} + \Delta\Big(\frac{x}{z},\mu^2\Big)L_q^{\rm NS}\Big(z,\frac{Q^2}{m^2},\frac{m^2}{\mu^2}\Big)\Big] \\ +\frac{1}{2}e_Q^2\int_x^{z_{\max}}\frac{dz}{z}\Big\{\Sigma\Big(\frac{x}{z},\mu^2\Big)H_q^{\rm PS}\Big(z,\frac{Q^2}{m^2},\frac{m^2}{\mu^2}\Big) \\ +G\Big(\frac{x}{z},\mu^2\Big)H_g^{\rm S}\Big(z,\frac{Q^2}{m^2},\frac{m^2}{\mu^2}\Big)\Big\}, \end{aligned} \tag{2.9}$$

where the upper boundary of the integration is given by $z_{\max} = Q^2/(4m^2 + Q^2)$. The function $G(z,\mu^2)$ stands for the polarized gluon density. The singlet combination of the polarized quark densities is defined by

$$\Sigma(z,\mu^2) = \sum_{i=1}^{n_f}\Big(f_i(z,\mu^2) + \overline{f}_i(z,\mu^2)\Big), \tag{2.10}$$

where f_i and $\overline{f}_i$ stand for the light quark and anti-quark densities of species i respectively. The non-singlet combination of the polarized quark densities is given by

$$\Delta(z,\mu^2) = \sum_{i=1}^{n_f}\Big(e_i^2 - \frac{1}{n_f}\sum_{k=1}^{n_f}e_k^2\Big)\Big(f_i(z,\mu^2) + \overline{f}_i(z,\mu^2)\Big). \tag{2.11}$$

In the above expressions the charges of the light quark and the heavy quark are denoted by e_i and e_Q respectively. Furthermore n_f stands for the number of light quarks and μ denotes the mass factorization scale, which we choose to be equal to the renormalization scale. The latter shows up in the running coupling constant denoted by $\alpha_s(\mu^2)$.

Like the parton densities the heavy quark coefficient functions L_i ($i = q, g$) can also be divided into singlet and non-singlet parts, which are indicated by the superscripts S and NS in (2.9). Furthermore the singlet quark coefficient function can be split into

$$L_q^{\rm S} = L_q^{\rm NS} + L_q^{\rm PS}. \tag{2.12}$$

The above relation originates from the light flavour decomposition of the Feynman graphs contributing to the structure function $g_1(x, Q^2, m^2)$ in (2.9). One class of graphs gives the same contributions to $L_q^{\rm S}$ as well as to $L_q^{\rm NS}$ whereas another class, which we call purely-singlet (PS), only contributes to $L_q^{\rm S}$. The latter class is characterized by those diagrams which have a gluon in the t-channel and can therefore only contribute to the singlet quark coefficient function $L_q^{\rm S}$. It turns out that up to order α_s^2 $L_q^{\rm S} = L_q^{\rm NS}$ and $L_g^{\rm S} = 0$. In the case of the heavy quark coefficient functions H_j there are no non-singlet parts and therefore $H_q^{\rm S} = H_q^{\rm PS}$. The latter gets contributions for the first time in order α_s^2, whereas the perturbation series in $H_g^{\rm S}$ starts in order α_s. The distinction between the heavy quark coefficient functions L_i and H_i can be traced back to the different photon-parton subprocesses from which they originate. The functions L_i are attributed to the reactions where the virtual photon couples to the light quark, whereas H_i originate from the reactions where the virtual photon couples to the heavy quark. Hence L_i and H_i in (2.9) are multiplied by e_i^2 and e_Q^2 respectively. Moreover when the reaction where the photon couples to the heavy quark contains a light quark in the initial state then it can only proceed via the exchange of a gluon in the t-channel between the light and heavy quark (see diagrams 5a, 5b in [14]). Therefore this process is purely singlet and there does not exist a non-singlet contribution to $H_q^{\rm S}$.

We will now discuss the various subprocesses which contribute to the spin dependent heavy quark coefficient function up to order α_s^2. Both the coefficient functions L_i and H_i can be expanded in a power series of $\alpha_s/(4\pi)$ with coefficients $L_i^{(n)}$, $H_i^{(n)}$ respectively, where n denotes the order in the perturbation series. Until now only the lowest order (LO) coefficient $H_g^{(1)}$ is exactly known and it is given by the photon-gluon fusion process

$$\gamma^*(q) + g(k_1) \to Q(p_1) + \overline{Q}(p_2)\,, \tag{2.13}$$

which yields the answer [11], [12], [13]

$$H_g^{(1)}(z, Q^2, m^2) = T_f\Big[4(2z-1)\ln\Big(\frac{1+sq_1}{1-sq_1}\Big) + 4(3-4z)sq_1\Big] \tag{2.14}$$

with

$$sq_1 = \sqrt{1 - \frac{4z}{(1-z)\xi}}\,, \quad \xi = \frac{Q^2}{m^2}\,, \quad z = \frac{Q^2}{2q\cdot k_1}\,. \tag{2.15}$$

where $0 < z < \xi/(\xi+4)$ and the colour factor $T_f = 1/2$ in SU(N). In NLO we encounter the following subprocesses. First we have the gluon bremsstrahlung subprocess

$$\gamma^*(q) + g(k_1) \to g(k_2) + Q(p_1) + \overline{Q}(p_2)\,. \tag{2.16}$$

Including the virtual gluon corrections to (2.13) we obtain the contribution $H_g^{(2)}$ which is not yet known and for which the asymptotic form in the limit $Q^2 \gg m^2$ will be determined in section 4. In addition to (2.16) we have the subprocess

$$\gamma^*(q) + q(\overline{q})(k_1) \to q(\overline{q})(k_2) + Q(p_1) + \overline{Q}(p_2)\,, \tag{2.17}$$

which can be subdivided into two different production mechanisms. The first one is given by the Bethe-Heitler process (see figs. 5a,b in [14]) and the second one can be attributed to the Compton reaction (see figs. 5c,d in [14]). In the case of the Bethe-Heitler process the virtual photon couples to the heavy quark and therefore this reaction leads to $H_q^{(2)}$. Like $H_g^{(2)}$ the coefficient function $H_q^{(2)}$ is not known and its asymptotic form will be presented in section 4. In the Compton reaction the virtual photon couples to the light (anti-) quark and its contribution to $L_q^{\rm NS}$ leads to $L_q^{\rm NS,(2)} = L_q^{\rm S,(2)}$ (see the discussion below (2.12)). Finally we want to make the comment that there are no interference terms between the Bethe-Heitler and Compton reactions in (2.17) if one integrates over all final state momenta.

Like in the unpolarized case the computation of the Compton process is rather trivial and we can present an exact form of $L_q^{\rm NS,(2)}$

$$\begin{aligned}
L_q^{\rm NS,(2)}(z,\frac{Q^2}{m^2},\frac{m^2}{\mu^2}) &= C_F T_f \Big[\Big\{\frac{4}{3}\frac{1+z^2}{1-z} - \frac{16z}{1-z}\Big(\frac{z}{\xi}\Big)^2\Big\}\Big\{\ln\Big(\frac{1-z}{z^2}\Big)L_1 \\
&+L_1L_2 + 2(-DIL1 + DIL2 + DIL3 - DIL4)\Big\} \\
&+\Big\{-\frac{8}{3} + \frac{4}{1-z} + \Big(\frac{z}{(1-z)\xi}\Big)^2\Big(-16 + 32z - \frac{8}{1-z}\Big)\Big\}L_1 \\
&+\Big\{\frac{64}{9} + \frac{112}{9}z - \frac{152}{9}\frac{1}{1-z} + \Big(\frac{z}{(1-z)\xi}\Big)\Big(\frac{512}{9} - \frac{128}{3}z + \frac{848}{9}z^2\Big) \\
&+\Big(\frac{z}{(1-z)\xi}\Big)^2\Big(-\frac{640}{9} + \frac{1408}{9}z - \frac{2368}{9}z^2 + \frac{1600}{9}z^3\Big)\Big\}\frac{L_3}{sq_2} \\
&+\Big\{-\frac{188}{27} - \frac{872}{27}z + \frac{718}{27}\frac{1}{1-z} + \Big(\frac{z}{(1-z)\xi}\Big)\Big(-\frac{952}{27} + \frac{1520}{27}z
\end{aligned}$$

$$-\frac{800}{9}z^2+\frac{20}{27}\frac{1}{1-z}\Big)\Big\}sq_1\Big]\,, \tag{2.18}$$

where sq_1 is defined in (2.15) and $C_F = (N^2-1)/(2N)$ in SU(N). Further we have defined

$$\begin{aligned}
sq_2 &= \sqrt{1-4\frac{z}{\xi}}\,,\\
L_1 = \ln\Big(\frac{1+sq_1}{1-sq_1}\Big) \quad &, \quad L_2 = \ln\Big(\frac{1+sq_2}{1-sq_2}\Big) \quad , \quad L_3 = \ln\Big(\frac{sq_2+sq_1}{sq_2-sq_1}\Big)\,,\\
DIL_1 = \mathrm{Li}_2\bigg(\frac{(1-z)(1+sq_1)}{1+sq_2}\bigg) \quad &, \quad DIL_2 = \mathrm{Li}_2\Big(\frac{1-sq_2}{1+sq_1}\Big)\,,\\
DIL_3 = \mathrm{Li}_2\Big(\frac{1-sq_1}{1+sq_2}\Big) \quad &, \quad DIL_4 = \mathrm{Li}_2\Big(\frac{1+sq_1}{1+sq_2}\Big)\,.
\end{aligned} \tag{2.19}$$

Here $\mathrm{Li}_2(x)$ is the dilogarithm defined in [19].

The derivation of the asymptotic formulae for the heavy quark coefficient functions has been given for the spin averaged structure functions F_L and F_2 in [15]. The procedure can be immediately carried over to the spin structure function g_1 and we only quote the results.

In the limit $Q^2 \gg m^2$ the heavy quark coefficient functions H_ℓ can be obtained as follows

$$H_\ell\Big(\frac{Q^2}{m^2},\frac{m^2}{\mu^2}\Big) = A_{k\ell}\Big(\frac{m^2}{\mu^2}\Big)\otimes C_k\Big(\frac{Q^2}{\mu^2}\Big)\,, \tag{2.20}$$

with $k,\ell = q,g$ and $\otimes$ denotes the convolution symbol

$$(f\otimes g)(z) = \int_0^1 dz_1\int_0^1 dz_2\,\delta(z-z_1z_2)f(z_1)g(z_2)\,. \tag{2.21}$$

Notice that for convenience we have suppressed the z-dependence in (2.20). The operator matrix elements (OME's) $A_{k\ell}$ are defined by

$$A_{k\ell}\Big(\frac{m^2}{\mu^2}\Big) = <\ell|O_k|\ell>\,, \tag{2.22}$$

where O_k $(k = q,g)$ are the composite quark and gluon operators which appear in the operator product expansion (OPE) of the electro-magnetic current in (2.2) near the light-cone (see e.g. eq.(2.22) in [15]). In (2.20) the

operators are already renormalized and sandwiched between on-shell light quark and gluon states indicated by $|\ell>$. The latter leads to collinear divergences which, however, are removed via mass factorization so that the $A_{k\ell}$ are finite. Finally the OME's contain one heavy quark loop only and they will be calculated up to $O(\alpha_s^2)$ in the next section. The objects C_k in (2.20) denote the light quark and gluon coefficient functions which contribute to the spin structure function g_1. They have been calculated up to second order in [20]. Notice that relation (2.20) also holds for the heavy quark coefficient functions of type L_l.

Finally we want to make the remark that, like in the case of the coefficient functions, the OME's can also be divided into non-singlet (NS), singlet (S) and purely-singlet (PS) parts. In particular we have the relation

$$A_{qq}^{\rm S} = A_{qq}^{\rm NS} + A_{qq}^{\rm PS}\,, \tag{2.23}$$

and the origin of $A_{qq}^{\rm PS}$ is the same as mentioned below (2.12) for the $L_q^{\rm PS}$ and $H_q^{\rm PS}$. Like in the case of $H_q^{\rm PS}$ the OME's $A_{qq}^{\rm PS}$ are determined by the graphs where two gluons are exchanged between the heavy quark and light quark so that only the singlet channel can contribute.

3 Calculation of the two-loop spin operator matrix elements

In this section we present the calculation of the spin dependent OME's in (2.22) containing one heavy quark loop up to two-loop order. A similar calculation has been carried out for the spin averaged (unpolarized) OME's in [15]. The calculation of the spin dependent OME's proceeds in an analogous way. The twist two operators O_q and O_g appearing in (2.22) are defined by

$$O_{q,r}^{\mu_1\cdots\mu_n}(x) = i^n S\Big[\overline{\psi}(x)\gamma_5\gamma^{\mu_1}D^{\mu_2}\cdots D^{\mu_n}\frac{\lambda_r}{2}\psi(x)\Big] + \text{trace terms}\,, \tag{3.1}$$

$$O_{q}^{\mu_1\cdots\mu_n}(x) = i^n S\Big[\overline{\psi}(x)\gamma_5\gamma^{\mu_1}D^{\mu_2}\cdots D^{\mu_n}\psi(x)\Big] + \text{trace terms}\,, \tag{3.2}$$

$$\begin{aligned} O_{g}^{\mu_1\cdots\mu_n}(x) = i^n S\Big[\frac{1}{2}\epsilon^{\mu_1\alpha\beta\gamma}\mathrm{Tr}\Big(F_{\beta\gamma}(x)D^{\mu_2}\cdots D^{\mu_{n-1}}F_{\alpha}^{\mu_n}(x)\Big)\Big] \\ +\text{trace terms}\,. \end{aligned} \tag{3.3}$$

The symbol S in front of the square bracket stands for the symmetrization of the Lorentz indices $\mu_1\cdots\mu_n$ where n denotes the spin of the operator. The above set of operators can be distinguished with respect to the flavour group $SU(n_f)$ in a non-singlet part (3.1), carrying the flavour group generator λ_r, and the singlet parts (3.2) and (3.3). The quark and the gluon field tensors are given by $\psi(x)$ and $F_{\mu\nu}^a(x)$ respectively with $F_{\mu\nu} = F_{\mu\nu}^a T^a$ where T^a stands for the generator of the colour group $SU(N)$ ($N = 3$). The covariant derivative is denoted by $D_\mu = \partial_\mu + ig\,T^a A_\mu^a(x)$ where $A_\mu^a(x)$ represents the gluon field. The operator vertices corresponding to the operators (3.1)$-$(3.3) can e.g. be found in appendix A of [21]. The heavy quark coefficient functions mentioned in the last section require the calculation of the following OME's (see (2.22)). Starting with the photon-gluon fusion reaction (2.13), (2.16) we have to compute up to second order

$$A_{Qg}^{\mathrm{S,(n)}}\Big(\frac{m^2}{\mu^2}\Big) =< g|O_Q^{(n)}(0)|g >\,, \tag{3.4}$$

where Q stands for the heavy quark with mass m. The OME's corresponding to (3.4) are determined by the Feynman graphs in fig. 1 (first order) and

fig. 2 (second order). For the Bethe-Heitler reaction (2.17), which starts in second order of α_s, we need

$$A_{Qq}^{\mathrm{PS},(n)}\Big(\frac{m^2}{\mu^2}\Big) =< q|O_Q^{(n)}(0)|q > \ . \tag{3.5}$$

Here the two-loop graphs are depicted in fig. 3. Finally we also want to obtain the asymptotic form of the coefficient function for the Compton reaction (2.17) presented in (2.18). For this we need to calculate

$$A_{qq,Q}^{\mathrm{NS},(n)}\Big(\frac{m^2}{\mu^2}\Big) =< q|O_q^{(n)}(0)|q > , \tag{3.6}$$

which is derived from the graphs in fig. 4 containing the heavy quark loop (Q) contribution to the gluon self-energy. Since the OME's $A_{k\ell}^{(n)}$ are S-matrix elements they originate from the Fourier transform in momentum space of the following connected Green's functions. The connected Green's function

$$< 0|T(A_\mu^a(x)O_Q^{\mu_1\cdots\mu_n}(0)A_\nu^b(y)|0 >_c , \tag{3.7}$$

corresponds to equation (3.4). Here $O_Q^{\mu_1\cdots\mu_n}$ stands for the heavy quark composite operator which is defined in the same way as in (3.2) except that now the Dirac field occurring in $O_Q^{\mu_1\cdots\mu_n}$ represents the heavy quark. The heavy quark composite operator can be also sandwiched between light quark fields denoted by $\psi_i(x)$

$$< 0|T(\overline{\psi}_i(x)O_Q^{\mu_1\cdots\mu_n}(0)\psi_j(y)|0 >_c , \tag{3.8}$$

which correspond to (3.5). Finally the connected Green's function related to (3.6) is given by

$$< 0|T(\overline{\psi}_i(x)O_{q,r}^{\mu_1\cdots\mu_n}(0)\psi_j(y)|0 >_c , \tag{3.9}$$

where again $\psi_i(x)$ represents the light quarks and $O_{q,r}^{\mu_1\cdots\mu_n}$ is the non-singlet light quark composite operator in (3.1). In these connected Green's functions a and i, j are the colour indices of the gluon field A_μ and the quark fields $\bar{\psi}$, ψ respectively. Before one obtains the S-matrix elements in (3.4)-(3.6) the external gluon and quark propagators appearing in (3.7)-(3.9) have to be amputated. Further one has to include the external quark and gluon

self-energies given by the graphs s, t in fig. 2. One can simplify the above connected Green's functions using the property that the composite operators are traceless symmetric tensors under the Lorentz group. Therefore one obtains many trace terms which are not essential for the determination of the OME's $A_{k\ell}^{(n)}$. These trace terms can be eliminated by multiplying the operators by an external source $J_{\mu_1\cdots\mu_n} = \Delta_{\mu_1}\cdots\Delta_{\mu_n}$ with $\Delta^2 = 0$. Performing the Fourier transform into momentum space and sandwiching the connected Green's function (3.7) by the external gluon polarization vectors $\epsilon^\mu(p)$, $\epsilon^\nu(p)$, one obtains

$$\epsilon^\mu(p) G^{ab}_{Q,\mu\nu} \epsilon^\nu(p)\,, \tag{3.10}$$

where p stands for the momentum of the external gluon in the graphs of figs. 1, 2 with $p^2 = 0$. The tensor $G^{ab}_{Q,\mu\nu}$ has the form

$$G^{ab}_{Q,\mu\nu} = \hat{A}^{\mathrm{S,(n)}}_{Qg}\Big(\epsilon, \frac{m^2}{\mu^2}, \alpha_s\Big)\delta^{ab}(\Delta.p)^{n-1}\epsilon_{\mu\nu\alpha\beta}\Delta^\alpha p^\beta\,. \tag{3.11}$$

Proceeding in the same way for the connected Green's functions in (3.8) and (3.9) after multiplication by the Dirac spinors $\bar{u}(\vec{p},s)$, $u(\vec{p},s)$ one obtains

$$\overline{u}(\vec{p},s) G^{ij}_Q u(\vec{p},s) \tag{3.12}$$

and

$$\overline{u}(\vec{p},s) G^{ij}_q \lambda_r u(\vec{p},s)\,, \tag{3.13}$$

respectively. Here λ_r denote the generators of the flavour group $SU(n_f)$ and $u(\vec{p},s)$ stands for the Dirac spinor corresponding to the light external quark in the graphs of figs. 3, 4 with momentum p ($p^2 = 0$). The tensors G^{ij}_Q and G^{ij}_q become equal to

$$G^{ij}_Q = \hat{A}^{PS,(n)}_{Qq}\Big(\epsilon, \frac{m^2}{\mu^2}, \alpha_s\Big)\delta^{ij}(\Delta.p)^{n-1}\not{\Delta}\gamma_5\,, \tag{3.14}$$

$$G^{ij}_q = \hat{A}^{NS,(n)}_{qq}\Big(\epsilon, \frac{m^2}{\mu^2}, \alpha_s\Big)\delta^{ij}(\Delta.p)^{n-1}\not{\Delta}\gamma_5\,. \tag{3.15}$$

Notice that the operators appearing in the connected Green's functions (3.7)$-$(3.9) are still unrenormalized so that the OME's $\hat{A}_{k\ell}$ contain ultraviolet (UV)

divergences. Besides the UV-singularities we also encounter collinear (C) divergences. They can be attributed to the coupling of massless external quarks and gluons in the graphs of figs. 2-4 to internal massless quanta. Both types of singularities have to be regularized and we choose the method of d-dimensional regularization. This regularization leads to pole terms of the type $1/\epsilon^i$ ($\epsilon = d-4$) in the unrenormalized quantities $\hat{A}_{k\ell}$ which have to be removed via renormalization and mass factorization. Sometimes it is useful to distinguish between UV- and C-divergences and, where appropriate, we will indicate them by the notation ϵ_{UV} and ϵ_C respectively in the subsequent formulae. In general d-dimensional regularization is the most suitable method to regularize all kinds of singularities appearing in perturbative quantum field theories since it preserves the Slavnov-Taylor identities characteristic of gauge field theories. However, in the case of spin quantities the γ_5-matrix appears together with the Levi-Civita tensor (see eqs.(3.10)-(3.15)) for which one has to find a d-dimensional prescription. For the γ_5-matrix we will choose the prescription of 't Hooft and Veltman [22] which is equivalent to the one given by Breitenlohner and Maison in [23]. Since in our calculations only one γ_5-matrix appears, one can show [24], [25] that the replacement of $\Delta\!\!\!/\gamma_5$ in (3.14), (3.15) by

$$\Delta\!\!\!/\gamma_5 = \frac{i}{6}\epsilon_{\mu\nu\rho\sigma}\Delta^\mu\gamma^\nu\gamma^\rho\gamma^\sigma \tag{3.16}$$

is equivalent to the prescription given in [22], [23]. Although the methods in [22]-[25] are all consistent they have one drawback, namely that the operator $O^\mu_{q,r}$(3.1) gets renormalized in spite of the fact that it is conserved. Furthermore the γ_5-prescription in (3.16) also affects $O^{\mu_1\cdots\mu_n}_{q,r}$ ($n>1$) (3.1) and $O^{\mu_1\cdots\mu_n}_{q}$(3.2) so that one has to introduce some additional renormalization constants to restore the Ward identities violated by (3.16). Unfortunately these constants have been only calculated in the literature [25] up to two-loop order for spin $n=1$ and we need the finite OME's $A^{(n)}_{k\ell}$ for arbitrary n. However, as we will show later on, one can avoid the last procedure as long as one combines quantities which are calculated using the same γ_5-prescription. This is what happens in the case of the heavy quark coefficient functions H_ℓ as presented in (2.20). If the OME's $A_{k\ell}$ and the light parton coefficient functions C_k are computed using the same definition for the γ_5-matrix and the Levi-Civita tensor the prescription dependence will cancel in the product on the right-hand side of (2.20) providing us with a unique result for H_ℓ.

The unrenormalized $\hat{A}_{Qg}^{(n)}$ in (3.11) can be obtained as follows. First one replaces the γ_5-matrix appearing in $O_Q^{\mu_1\cdots\mu_n}$ in (3.7) according to prescription (3.16). Because of Lorentz covariance the Levi-Civita tensor in (3.11) emerges in a natural way. This tensor can be projected out in d-dimensions using the relation

$$\hat{A}_{Qg}^{\mathrm{S},(\mathrm{n})}\Big(\epsilon, \frac{m^2}{\mu^2}, \alpha_s\Big) = \frac{1}{N^2-1}\frac{1}{(d-2)(d-3)}\epsilon^{\mu\nu\lambda\sigma}\delta^{ab}(\Delta.p)^{-n}G^{ab}_{Q,\mu\nu}\Delta_\lambda p_\sigma \,. \quad (3.17)$$

In this way we obtain only Lorentz scalars in the numerators of the Feynman integrals which can be partially cancelled by similar terms appearing in the denominators. The traces of the Feynman loops in figs. 1, 2 and the contractions over dummy Lorentz indices have been performed with the algebraic manipulation program FORM [26]. The calculation of many of the scalar integrals has been already done in [15] for the spin averaged analogue of $\hat{A}_{Qg}^{(n)}$ and we can take over those results except for some additional integrals which we have computed for the spin case in (3.17). In the discussion of our results we will drop the S in $A_{Qg}^{\mathrm{S},(\mathrm{n})}$ and perform the inverse Mellin transformation on the OME's so that they become dependent on the partonic variable z in (2.15). This implies that all the products are replaced by convolutions according to (2.21).

The one-loop OME $\hat{A}_{Qg}^{(1)}$, which only gets a non-zero contribution from diagram a in fig. 1, can be cast in the algebraic form

$$\hat{A}_{Qg}^{(1)} = S_\epsilon\Big(\frac{m^2}{\mu^2}\Big)^{\epsilon/2}\Big\{ -\frac{1}{\epsilon_{\rm UV}}P_{qg}^{(0)} + a_{Qg}^{(1)} + \epsilon_{\rm UV}\bar{a}_{Qg}^{(1)}\Big\}\,. \quad (3.18)$$

Here S_ϵ is a spherical factor defined by

$$S_\epsilon = \exp\Big\{\frac{\epsilon}{2}\Big[\gamma_E - \ln(4\pi)\Big]\Big\}\,, \quad (3.19)$$

which is characteristic of d-dimensional regularization and contains the Euler constant γ_E. The mass parameter μ originates from the dimensionality of the coupling constant g ($\alpha_s = g^2/(4\pi)$) in d-dimensions and should not be confused with the renormalization and mass factorization scales. However, if one only subtracts the pole terms like in the $\overline{\rm MS}$-scheme, the mass parameter μ turns into the afore-mentioned scales. The superscript k in $\hat{A}_{ij}^{(k)}$ denotes

the order in the perturbation series expansion of the OME's which can be written as

$$\hat{A}_{ij} = \sum_{k=0}^{\infty} \Big(\frac{\alpha_s}{4\pi}\Big)^k \hat{A}_{ij}^{(k)} \,. \tag{3.20}$$

The objects $P_{ij}^{(k)}$ $(i,j = q,g; k = 0,1,\cdots)$ which we will need for (3.18) and the subsequent expressions denote the spin AP-splitting functions which have been calculated up to next-to-leading order in [21], [27]. In lowest order the renormalization group coefficients in (3.18) become

$$\begin{aligned} P_{qg}^{(0)} &= 8T_f[2z-1] \\ a_{Qg}^{(1)} &= 0 \\ \overline{a}_{Qg}^{(1)} &= -\frac{1}{8}\zeta(2) P_{qg}^{(0)} \,. \end{aligned} \tag{3.21}$$

The two-loop OME $\hat{A}_{Qg}^{(2)}$ which is determined by the graphs in fig. 2 is given by $(A.1)$. As has been shown in section 3 of [15], it can be expressed into the renormalization group coefficients as follows

$$\begin{aligned} \hat{A}_{Qg}^{(2)} = S_\epsilon^2 \Big(\frac{m^2}{\mu^2}\Big)^\epsilon \Big[\frac{1}{\epsilon^2} \Big\{ \frac{1}{2} P_{qg}^{(0)} \otimes (P_{qq}^{(0)} - P_{gg}^{(0)}) + \beta_0 P_{qg}^{(0)} \Big\} \\ + \frac{1}{\epsilon} \Big\{ -\frac{1}{2} P_{qg}^{(1)} - 2\beta_0 a_{Qg}^{(1)} - a_{Qg}^{(1)} \otimes (P_{qq}^{(0)} - P_{gg}^{(0)}) \Big\} + a_{Qg}^{(2)} \Big] \\ - \frac{2}{\epsilon} S_\epsilon \sum_{H=Q}^{t} \beta_{0,H} \Big(\frac{m_H^2}{\mu^2}\Big)^{\epsilon/2} \Big(1 + \frac{1}{8}\epsilon^2 \zeta(2)\Big) \hat{A}_{Qg}^{(1)} \,. \end{aligned} \tag{3.22}$$

In the above expression, where mass renormalization has already been carried out, the pole terms ϵ^{-k} stand for the UV as well as C-divergences so that we have put $\epsilon_{UV} = \epsilon_C$. The last term in (3.22) can be traced back to the graphs s, t in fig. 2. which contain the heavy quark loop contributions to the external gluon self-energy. Here one sums over all heavy quarks called H starting with $H = Q$ and ending with $H = t$ (top-quark). Notice that Q is the lightest heavy quark which is the same as the one produced in the final state of process (2.1). Further it also appears in the heavy quark operator whose OME's are shown in figs. 1, 2. For instance for charm production in (2.1) we have $Q = c$, $m_c = m$ and the sum in (3.22) runs over $H = c, b, t$. In

the case of bottom (b) production we have $Q = b$, $m_b = m$ and the sum runs over $H = b, t$. The contribution to the beta-function from a heavy quark H is given by

$$\beta_{0,H} = -\frac{4}{3} T_f \,, \tag{3.23}$$

for all species H which implies that $\beta_{0,Q} = \beta_{0,H}$. The Riemann zeta-function $\zeta(2) = \pi^2/6$ originates from the heavy quark contribution to the gluon self-energy denoted by $\Pi(p^2, m^2)$. At $p^2 = 0$ the unrenormalized expression $\Pi(0, m^2)$ is proportional to $(1 + \epsilon^2 \zeta(2)/8)/\epsilon$.

The other renormalization group coefficients can be inferred from the literature [21], [27]-[29] and they are given by

$$\begin{aligned}
\beta_0 &= \frac{11}{3} C_A - \frac{4}{3} n_f T_f \,, \\
P_{qq}^{(0)} &= 4 C_F \Big[2 \Big(\frac{1}{1-z} \Big)_+ - 1 - z + \frac{3}{2} \delta(1-z) \Big] \,, \\
P_{gg}^{(0)} &= 8 C_A \Big[\Big(\frac{1}{1-z} \Big)_+ + 1 - 2z \Big] + 2 \beta_0 \delta(1-z) \,, \\
P_{qg}^{(1)} &= 4 C_F T_f \Big[2(1-2z) \Big(-2 \ln^2(1-z) + 4 \ln z \ln(1-z) - \ln^2 z + 4 \zeta(2) \Big) \\
&\quad + 16(1-z) \ln(1-z) - 2(1-16z) \ln z + 4 + 6z \Big] \\
&\quad + 4 C_A T_f \Big[4(1-2z) \ln^2(1-z) - 4(1+2z) \Big(\ln^2 z + 2 \ln z \ln(1+z) \\
&\quad + 2 \mathrm{Li}_2(-z) \Big) - 8 \zeta(2) + 4(1+8z) \ln z - 16(1-z) \ln(1-z) \\
&\quad + 4(12 - 11z) \Big] \,,
\end{aligned} \tag{3.24}$$

where the colour factor C_A is given by $C_A = N$ in SU(N).

The full analytic expression for the unrenormalized $\hat{A}_{Qg}^{(2)}$ can be found in (A.1). Here the polylogarithmic functions $\mathrm{Li}_n(z)$ and $\mathrm{S}_{n,p}(z)$ are defined in [19]. In order to construct the heavy quark coefficient functions in the next section we need to renormalize $\hat{A}_{Qg}^{(\ell)}$ ($\ell = 0, 1$) in eqs. (3.18) and (3.22). For the coupling constant renormalization we choose a scheme where the

heavy quarks H appearing in the sum of (3.22) decouple from the running coupling constant $\alpha_s(\mu^2)$ when $\mu^2 < m_H^2$. This renormalization prescription completely removes the last term in (3.22) from the OME $\hat{A}_{Qg}^{(2)}$. It also implies that only the light flavours indicated by n_f appear in the running coupling constant. For instance in the case of charm production $n_f = 3$ and the c, b and t quark contributions are absent in the running coupling constant.

Furthermore one has to remove the C-divergences occurring in (3.22) via mass factorization. The above procedure has been carried out in section 3 of [15] in the context of the spin averaged OME and we can simply take over the algebraic expressions from that paper. In the $\overline{\rm MS}$-scheme the renormalized OME's $A_{Qg}^{(1)}$ and $A_{Qg}^{(2)}$ become

$$A_{Qg}^{(1)} = -\frac{1}{2} P_{qg}^{(0)} \ln \frac{m^2}{\mu^2} + a_{Qg}^{(1)}\,, \tag{3.25}$$

$$\begin{aligned} A_{Qg}^{(2)} = &\Big\{\frac{1}{8} P_{qg}^{(0)} \otimes (P_{qq}^{(0)} - P_{gg}^{(0)}) + \frac{1}{4}\beta_0 P_{qg}^{(0)}\Big\} \ln^2 \frac{m^2}{\mu^2} \\ &+\Big\{ -\frac{1}{2} P_{qg}^{(1)} - \beta_0 a_{Qg}^{(1)} + \frac{1}{2} a_{Qg}^{(1)} \otimes (P_{gg}^{(0)} - P_{qq}^{(0)})\Big\} \ln \frac{m^2}{\mu^2} \\ &+a_{Qg}^{(2)} + 2\beta_0 \bar{a}_{Qg}^{(1)} + \bar{a}_{Qg}^{(1)} \otimes (P_{qq}^{(0)} - P_{gg}^{(0)})\,. \end{aligned} \tag{3.26}$$

Notice that (3.26) is still dependent on the γ_5-matrix prescription which enters the $C_F T_f$ part (see (A.1)). This is exhibited by the splitting function $P_{qg}^{(1)}$ (3.24) where the $C_F T_f$ part still has to undergo an additional renormalization in order to become equal to the result in [21], [27]. The prescription dependence also affects $a_{Qg}^{(2)}$. However as will be shown in the next section this will be compensated in the construction of the heavy quark coefficient functions when we add the same type of term coming from the massless parton coefficient function $C_g^{(2)}$ computed in [20].

Finally, the unrenormalized as well as renormalized OME's $A_{Qg}^{(\ell)}$ ($\ell = 1, 2$) satisfy the relation

$$\int_0^1 dz\; A_{Qg}^{(\ell)}(z) = 0\,. \tag{3.27}$$

The OME $A_{Qq}^{\rm PS,(2)}$ is determined by the graphs in fig. 3. However it appears that only diagram a gives a nonzero contribution. The easiest way to compute

this graph is by using the standard Feynman parameterization which provides us with (see (3.14)) the unrenormalized OME

$$\hat{A}_{Qq}^{\mathrm{PS},(2)} = S_\epsilon^2 \Big(\frac{m^2}{\mu^2}\Big)^\epsilon \Big[\frac{1}{\epsilon^2}\{-\frac{1}{2}P_{qg}^{(0)} \otimes P_{gq}^{(0)}\} + \frac{1}{\epsilon}\{-\frac{1}{2}P_{qq}^{\mathrm{PS},(1)} + a_{Qg}^{(1)} \otimes P_{gq}^{(0)}\} + a_{Qq}^{\mathrm{PS},(2)}\Big] . \tag{3.28}$$

Like in the case of $\hat{A}_{Qg}^{(2)}$ (3.22) we did not make any distinction between UV- and C-singular pole terms ϵ^{-k} ($\epsilon_{\mathrm{UV}} = \epsilon_{\mathrm{C}}$). The renormalization group coefficients are given by (see also (3.21))

$$P_{gq}^{(0)} = 4C_F[2 - z] ,$$

$$P_{qq}^{\mathrm{PS},(1)} = 16C_F T_f[-(1+z)\ln^2 z - (1-3z)\ln z + 1 - z] . \tag{3.29}$$

The analytic expression for the unrenormalized $\hat{A}_{Qq}^{\mathrm{PS},(2)}$ can be found in (A.2). After removing the UV- and C-divergences the renormalized OME reads (see section 3 of [15])

$$A_{Qq}^{\mathrm{PS},(2)} = \Big\{ -\frac{1}{8}P_{qg}^{(0)} \otimes P_{gq}^{(0)}\Big\} \ln^2 \frac{m^2}{\mu^2} + \Big\{ -\frac{1}{2}P_{qq}^{\mathrm{PS},(1)} + \frac{1}{2}a_{Qg}^{(1)} \otimes P_{gq}^{(0)}\Big\} \ln \frac{m^2}{\mu^2} + a_{Qq}^{\mathrm{PS},(2)} - \bar{a}_{Qg}^{(1)} \otimes P_{gq}^{(0)} . \tag{3.30}$$

The above expression is represented in the $\overline{\mathrm{MS}}$-scheme. Like $A_{Qg}^{(2)}$ in (3.26), $A_{Qq}^{\mathrm{PS},(2)}$ still depends on the prescription for the γ_5 matrix. Since $P_{qq}^{\mathrm{PS},(1)}$ already agrees with the results in [21], [27] it does not need any finite renormalization and the dependence on the prescription for the γ_5 matrix only enters via the non-logarithmic term $a_{Qq}^{\mathrm{PS},(2)}$. While computing the heavy quark coefficient function the latter dependence will be cancelled by contributions from the massless quark coefficient function $C_q^{\mathrm{PS},(2)}$ in [20].

Finally we call attention to the non-singlet OME $A_{qq,Q}^{\mathrm{NS},(2)}$ derived from the graphs in fig. 4. These graphs are also computed by Feynman parameteri-

zation and we get the unrenormalized result from (3.15)

$$\hat{A}^{\mathrm{NS},(2)}_{qq,Q} = S^2_\epsilon \Big(\frac{m^2}{\mu^2}\Big)^\epsilon \Big[\frac{1}{\epsilon^2_{\mathrm{UV}}}\Big\{ -\beta_{0,Q} P^{(0)}_{qq}\Big\} + \frac{1}{\epsilon}\Big\{ -\frac{1}{2} P^{\mathrm{NS},(1)}_{qq,Q}\Big\} + a^{\mathrm{NS}(2)}_{qq,Q}\Big] . \tag{3.31}$$

Notice that in fig. 4 the heavy flavour loop contribution to the gluon self-energy, denoted by $\Pi(p^2, m^2)$, contains the heavy quark Q with mass m only. For the construction of the heavy quark coefficient function $L^{(2)}_q$ we do not need the contribution of the other heavy quarks (as mentioned below (3.22)) which have masses larger than m. Contrary to $\hat{A}^{(2)}_{Qg}$ and $\hat{A}^{\mathrm{PS},(2)}_{Qq}$ the above equation only contains UV-divergences since the heavy quark Q prevents $\hat{A}^{\mathrm{NS},(2)}_{qq,Q}$ from being C-singular provided that the gluon self-energy is renormalized in such a way that $\Pi_{\mathrm{R}}(0, m^2) = 0$. Further in the non-singlet case we can completely remove the dependence on the prescription for the γ_5-matrix since after renormalization $(A^{\mathrm{NS}}_{qq})_{\mathrm{spin}} = (A^{\mathrm{NS}}_{qq})_{\mathrm{spin\ ave}}$. This has to be so because the splitting function P^{NS}_{qq} is the same for the spin averaged and the spin dependent non-singlet operators (see [21], [25], [27]). Therefore after removing the γ_5 prescription dependence $\hat{A}^{\mathrm{NS},(2)}_{qq,Q}$ becomes the same as in the spin averaged case and we get

$$\begin{aligned}
\beta_{0,Q} &= -\frac{4}{3} T_f \,, \\
P^{\mathrm{NS},(1)}_{qq,Q} &= C_F T_f \Big[-\frac{160}{9}\Big(\frac{1}{1-z}\Big)_+ + \frac{176}{9} z - \frac{16}{9} \\
&\quad - \frac{16}{3}\frac{1+z^2}{1-z}\ln z + \delta(1-z)\Big(-\frac{4}{3} - \frac{32}{3}\zeta(2)\Big)\Big] .
\end{aligned} \tag{3.32}$$

The analytical expression for $\hat{A}^{\mathrm{NS},(2)}_{qq,Q}$ can be found in (C.5), (C.6) of [15]. After renormalization the OME becomes

$$A^{\mathrm{NS},(2)}_{qq,Q} = \Big\{ -\frac{1}{4}\beta_{0,Q} P^{(0)}_{qq}\Big\} \ln^2 \frac{m^2}{\mu^2} + \Big\{ -\frac{1}{2} P^{\mathrm{NS},(1)}_{qq,Q}\Big\} \ln \frac{m^2}{\mu^2} + a^{\mathrm{NS},(2)}_{qq,Q} + \frac{1}{4}\beta_{0,Q}\zeta(2) P^{(0)}_{qq} \,. \tag{3.33}$$

Summarizing our above results for the OME's we found that the coefficients of the double and single pole terms can be inferred from the AP

splitting functions and the beta-function which are published in the literature. In this way we have a check on the calculations of $\hat{A}_{ij}$. The non-pole terms $a_{Qg}^{(2)}$ (3.26) $a_{Qq}^{\mathrm{PS},(2)}$ (3.30) and $a_{qq,Q}^{\mathrm{NS},(2)}$ (3.33) cannot be predicted and are calculated in this paper. They are needed to compute the order α_s^2 spin-dependent heavy quark coefficient functions (2.20) up to the non-logarithmic term which will be done in the next section.

4 Heavy quark coefficient functions

In this section we present the heavy quark coefficient functions H_ℓ and L_ℓ ($\ell = q, g$) defined in (2.9) up to order α_s^2 in the asymptotic limit $Q^2 \gg m^2$. In [15] we showed that, for the spin averaged case, the asymptotic limits for H_ℓ and L_ℓ can be expressed into the renormalization group coefficients appearing in the algebraic expression for the OME's $A_{k\ell}$ and the massless parton coefficient functions C_k. This derivation follows from the mass factorization theorem, which is also applicable to the spin structure function $g_1(x, Q^2)$ in (2.9). The theorem states that the mass dependent terms of the type $\ln^i(m^2/\mu^2)\ln^j(Q^2/m^2)$ occurring in the asymptotic expressions for H_ℓ, L_ℓ can be factorized out in the following way

$$H_\ell^{\rm S}\Big(\frac{Q^2}{m^2}, \frac{m^2}{\mu^2}\Big) = A_{kl}^{\rm S}\Big(\frac{m^2}{\mu^2}\Big) \otimes C_k^{\rm S}\Big(\frac{Q^2}{\mu^2}\Big)\,, \tag{4.1}$$

$$L_\ell^{r}\Big(\frac{Q^2}{m^2}, \frac{m^2}{\mu^2}\Big) = A_{kl}^{r}\Big(\frac{m^2}{\mu^2}\Big) \otimes C_k^{r}\Big(\frac{Q^2}{\mu^2}\Big)\,, \tag{4.2}$$

where H_ℓ, L_ℓ ($\ell = q, g$) denote the spin dependent heavy quark coefficient functions in the limit $Q^2 \gg m^2$ and r =S, NS. Up to order α_s^2 the finite spin dependent OME's $A_{k\ell}$ ($k, \ell = q, g$) have been calculated in section 3 and are given in Appendix A. The spin dependent light parton coefficient functions C_k have been also calculated up to order α_s^2 and they can be found in [20]. Notice that $A_{k\ell}$ as well as C_k have been computed in the $\overline{\rm MS}$-scheme and in the case of (4.1) both depend on the prescription for the γ_5-matrix. In the products appearing on the right hand sides of (4.1), (4.2) the scheme dependence is only partially cancelled, which is revealed by the dependence of H_ℓ, L_ℓ on the factorization scale μ^2. The latter originates from the coupling of a light parton (gluon or quark) to an internal light parton which appears in subprocesses (2.16), (2.17). Fortunately the γ_5-matrix prescription cancels in the product on the right hand side of (4.1) as we will discuss below. Since the algebraic structure of the spin dependent heavy quark coefficient functions corresponding to $g_1(x, Q^2)$ in (2.9) is the same as derived for the spin averaged structure function $F_2(x, Q^2)$ we can simply take over the formulae in [15]. For the LO photon-gluon fusion process (2.13) we obtain

$$H_g^{(1)}\Big(\frac{Q^2}{m^2}, \frac{m^2}{\mu^2}\Big) = \frac{1}{2}P_{qg}^{(0)} \ln\frac{Q^2}{m^2} + a_{Qg}^{(1)} + c_g^{(1)}\,, \tag{4.3}$$

where $P_{qg}^{(0)}$ and $a_{Qg}^{(1)}$ appear in $A_{Qg}^{(1)}$ (3.25) and $c_g^{(1)}$ is the non-log term in the lowest order coefficient function defined by (see [20])

$$C_g^{(1)}\Big(\frac{Q^2}{\mu^2}\Big) = \frac{1}{2}P_{qg}^{(0)} \ln\frac{Q^2}{\mu^2} + c_g^{(1)}\,. \tag{4.4}$$

Notice that like $A_{k\ell}$ in (3.20) the coefficient functions are expanded as

$$C_k\Big(\frac{Q^2}{\mu^2}\Big) = \sum_{\ell=0}^{\infty}\Big(\frac{\alpha_s}{4\pi}\Big)^{\ell} C_k^{(\ell)}\Big(\frac{Q^2}{\mu^2}\Big)\,. \tag{4.5}$$

The explicit expression for (4.3) can be found in $(B.1)$. In NLO the spin dependent heavy quark coefficient function of the photon-gluon fusion process (2.13), (2.16) becomes

$$\begin{aligned}
H_g^{(2)}\Big(\frac{Q^2}{m^2},\frac{m^2}{\mu^2}\Big) &= \Big\{\frac{1}{8}P_{qg}^{(0)}\otimes(P_{gg}^{(0)}+P_{qq}^{(0)}) - \frac{1}{4}\beta_0 P_{qg}^{(0)}\Big\}\ln^2\frac{Q^2}{m^2}\\
&+\Big\{\frac{1}{2}P_{qg}^{(1)} - \beta_0 c_g^{(1)} + \frac{1}{2}P_{qq}^{(0)}\otimes a_{Qg}^{(1)} + \frac{1}{2}P_{gg}^{(0)}\otimes c_g^{(1)} + \frac{1}{2}P_{qg}^{(0)}\otimes c_q^{(1)}\Big\}\\
&\times\ln\frac{Q^2}{m^2} + \Big\{\frac{1}{4}P_{qg}^{(0)}\otimes P_{gg}^{(0)} - \frac{1}{2}\beta_0 P_{qg}^{(0)}\Big\}\ln\frac{Q^2}{m^2}\ln\frac{m^2}{\mu^2}\\
&+\Big\{-\beta_0(c_g^{(1)}+a_{Qg}^{(1)}) + \frac{1}{2}P_{gg}^{(0)}\otimes(c_g^{(1)}+a_{Qg}^{(1)})\Big\}\ln\frac{m^2}{\mu^2}\\
&+c_g^{(2)} + a_{Qg}^{(2)} + 2\beta_0\bar{a}_{Qg}^{(1)} + c_q^{(1)}\otimes a_{Qg}^{(1)} + P_{qq}^{(0)}\otimes\bar{a}_{Qg}^{(1)} - P_{gg}^{(0)}\otimes\bar{a}_{Qg}^{(1)}\,,
\end{aligned} \tag{4.6}$$

where the coefficients $P_{qg}^{(1)}$, $P_{ij}^{(0)}$, $a_{Qg}^{(\ell)}$, $\bar{a}_{Qg}^{(\ell)}$ show up in $A_{Qg}^{(2)}$ (3.26). The coefficients $c_g^{(\ell)}$ $(\ell = 1, 2)$ show up in the order α_s^2 contribution to the gluon coefficient function calculated in [20]. The latter can be written as

$$\begin{aligned}
C_g^{(2)}\Big(\frac{Q^2}{\mu^2}\Big) &= \Big\{\frac{1}{8}P_{qg}^{(0)}\otimes(P_{gg}^{(0)}+P_{qq}^{(0)}) - \frac{1}{4}\beta_0 P_{qg}^{(0)}\Big\}\ln^2\frac{Q^2}{\mu^2}\\
&+\Big\{\frac{1}{2}P_{qg}^{(1)} - \beta_0 c_g^{(1)} + \frac{1}{2}P_{gg}^{(0)}\otimes c_g^{(1)} + \frac{1}{2}P_{qg}^{(0)}\otimes c_q^{(1)}\Big\}\ln\frac{Q^2}{\mu^2}\\
&+c_g^{(2)}\,.
\end{aligned} \tag{4.7}$$

The explicit expression for (4.6) is given in $(B.2)$. The latter can be split into $C_F T_f$ and $C_A T_f$ parts (see (B.2)). The $C_A T_f$ part still depends on the

mass factorization scale μ^2 and is therefore scheme dependent (in our case the $\overline{\rm MS}$-scheme).

The same scale dependence was also found for the exact expression of $H_g^{(2)}$ (4.6) in [14]. It can be attributed to the coupling constant renormalization represented by the lowest order coefficient β_0 in the beta-function and to mass factorization which is revealed by the lowest order splitting function $P_{gg}^{(0)}$. The $C_F T_f$ part of $H_g^{(2)}$ is scheme independent which implies that it is obtained without performing renormalization and mass factorization on the original parton cross section of the photon-gluon fusion process (2.13), (2.16). Therefore the latter did not contain UV and C-divergences and it can be computed in four dimensions. From section 3 and [20] we infer that the prescription dependence of the γ_5-matrix only enters in the $C_F T_f$ parts of $A_{Qg}^{(2)}$ (3.26) and $C_g^{(2)}$ (4.7). Hence it has to cancel in the same part of $H_g^{(2)}$ because the latter can be computed in four dimensions, where the γ_5-matrix is unique. Further we made an interesting observation for the gluonic coefficient functions H_g and C_g (see [20]) i.e,

$$\int_0^1 dz\; H_g^{(\ell)}(z, \frac{Q^2}{m^2}, \frac{m^2}{\mu^2}) = 0\,, \qquad \int_0^1 dz\; C_g^{(\ell)}(z, \frac{Q^2}{\mu^2}) = 0\,, \tag{4.8}$$

with $\ell = 1, 2$. This property was already mentioned for $A_{Qg}^{(\ell)}$ (see (3.27)).

The asymptotic expression of the order α_s^2 spin dependent heavy quark coefficient function corresponding to the Bethe-Heitler process in (2.17) is given by

$$\begin{aligned} H_q^{(2)}(\frac{Q^2}{m^2}, \frac{m^2}{\mu^2}) = &\Big\{\frac{1}{8} P_{qg}^{(0)} \otimes P_{gq}^{(0)}\Big\} \ln^2 \frac{Q^2}{m^2} + \Big\{\frac{1}{2} P_{qq}^{\rm PS,(1)} + \frac{1}{2} P_{gq}^{(0)} \otimes c_g^{(1)}\Big\} \ln \frac{Q^2}{m^2} \\ &+\Big\{\frac{1}{4} P_{qg}^{(0)} \otimes P_{gq}^{(0)}\Big\} \ln \frac{Q^2}{m^2} \ln \frac{m^2}{\mu^2} + \Big\{\frac{1}{2} P_{gq}^{(0)} \otimes (c_g^{(1)} + a_{Qg}^{(1)})\Big\} \ln \frac{m^2}{\mu^2} \\ &+c_q^{\rm PS,(2)} + a_{Qq}^{\rm PS,(2)} - P_{gq}^{(0)} \otimes \bar{a}_{Qg}^{(1)}\,. \end{aligned} \tag{4.9}$$

The coefficients $P_{qq}^{\rm PS,(1)}$, $P_{ij}^{(0)}$, $a_{Qq}^{\rm PS,(2)}$ and $\bar{a}_{Qg}^{(1)}$ show up in $A_{Qq}^{\rm PS,(2)}$ (3.30) and $C_q^{\rm PS,(2)}$ appears in the pure singlet quark coefficient function calculated in [20]

$$C_q^{\rm PS,(2)}\Big(\frac{Q^2}{\mu^2}\Big) = \Big\{\frac{1}{8} P_{qg}^{(0)} \otimes P_{gq}^{(0)}\Big\} \ln^2 \frac{Q^2}{\mu^2}$$

$$+\Big\{\frac{1}{2}P_{qq}^{\mathrm{PS},(1)}+\frac{1}{2}P_{gq}^{(0)}\otimes c_g^{(1)}\Big\}\ln\frac{Q^2}{\mu^2}+c_q^{\mathrm{PS},(2)}\,. \tag{4.10}$$

The explicit expression for (4.9) can be found in (B.3). Notice that $H_q^{(2)}$ is still scheme dependent (in our case the $\overline{\mathrm{MS}}$ scheme), which is indicated by the mass factorization scale μ^2. This factorization scheme dependence shows up via the splitting function $P_{gq}^{(0)}$. The γ_5-matrix prescription dependence enters via the nonlogarithmic terms in $A_{Qq}^{\mathrm{PS},(2)}$ (3.30) as well as in $C_q^{\mathrm{PS},(2)}$ (4.10) and therefore cancels in the sum of both which equals $H_q^{(2)}$.

Finally we turn our attention to the Compton process in (2.17) which provides us with the spin dependent coefficient function L_q^{NS}. As can be inferred from (2.18) it is scheme independent since there is no dependence on μ^2. Furthermore the prescription dependence for the γ_5-matrix could be removed from $A_{qq,Q}^{\mathrm{NS},(2)}$ as well as from the order α_s^2 non-singlet coefficient function $C_{q,Q}^{\mathrm{NS},(2)}$. The latter reads (see (4.27) in [15])

$$\begin{aligned}C_{q,Q}^{\mathrm{NS},(2)}\Big(\frac{Q^2}{\mu^2},\frac{m^2}{\mu^2}\Big) &= \Big\{-\frac{1}{4}\beta_{0,Q}P_{qq}^{(0)}\Big\}\ln^2\frac{Q^2}{m^2}\\ &+\Big\{\frac{1}{4}\beta_{0,Q}P_{qq}^{(0)}\Big\}\ln^2\frac{m^2}{\mu^2}+\frac{1}{2}P_{qq,Q}^{\mathrm{NS},(1)}\ln\frac{Q^2}{\mu^2}\\ &-\beta_{0,Q}c_q^{(1)}\ln\frac{Q^2}{m^2}+c_{q,Q}^{\mathrm{NS},(2)}\,.\end{aligned} \tag{4.11}$$

In the above expression we have chosen the same renormalization for the heavy quark loop (Q) contribution to the gluon self-energy as the one appearing in the OME $A_{qq,Q}^{\mathrm{NS},(2)}$ (see below (3.31)). Finally the heavy quark coefficient function is given by

$$\begin{aligned}L_q^{\mathrm{NS},(2)}\Big(\frac{Q^2}{\mu^2},\frac{m^2}{\mu^2}\Big) &= \Big\{-\frac{1}{4}\beta_{0,Q}P_{qq}^{(0)}\Big\}\ln^2\frac{Q^2}{m^2}\\ &+\Big\{\frac{1}{2}P_{qq,Q}^{\mathrm{NS},(1)}-\beta_{0,Q}c_q^{(1)}\Big\}\ln\frac{Q^2}{m^2}+c_{q,Q}^{\mathrm{NS},(2)}+a_{qq,Q}^{\mathrm{NS},(2)}\\ &+\frac{1}{4}\beta_{0,Q}\zeta(2)P_{qq}^{(0)}\,,\end{aligned} \tag{4.12}$$

where the coefficients $P_{qq,Q}^{\mathrm{NS},(1)}$, $P_{qq}^{(0)}$, $\beta_{0,Q}$ and $a_{qq,Q}^{\mathrm{NS},(2)}$ show up in $A_{qq,Q}^{\mathrm{NS},(2)}$ (3.33). The coefficient $c_{q,Q}^{\mathrm{NS},(2)}$ can be found in [20]. The explicit expression for (4.12)

can be found in (B.4). One can check that in the limit $Q^2 \gg m^2$ the exact expression for the Compton process in (2.18) becomes equal to the asymptotic formula in (4.12) or in (B.4).

5 Results

In this section we compute the heavy charm component of the spin structure function $g_1(x,Q^2)$ and compare it with the light parton contributions. As has been mentioned before (see section 2) the order α_s spin dependent heavy quark coefficient function $H_g^{(1)}$ (2.14) is exactly known whereas the order α_s^2 coefficient functions computed in section 4 are only valid when $Q^2 \gg m^2$. Therefore the latter can only be used at those Q^2-values which are characteristic for the polarized electron and proton beam facility at HERA [7], [8]. If we want to use the asymptotic expressions at the lower Q^2-values, which are typical for the SMC-experiment [6], we have to improve them. To this purpose we will construct below some improved coefficient functions which can be also used at smaller Q^2-values. To check the validity of this approximation we carry out the same procedure for the spin averaged structure function $F_2(x,Q^2,m^2)$. The latter is expressed in parton densities and coefficient functions in the same way as done for $g_1(x,Q^2,m^2)$ in (2.9). The heavy quark coefficient functions needed for both g_1 and F_2 start in the same order of α_s and they have the same asymptotic behaviour exhibited by the large logarithmic terms $\ln^i(m^2/\mu^2)\ln^j(Q^2/m^2)$. Further the spin averaged as well as the spin dependent $H_g^{(2)}$ show the same threshold behaviour which is determined by soft gluon bremsstrahlung [16], [17]. However contrary to g_1 the exact heavy quark coefficient functions are known for F_2 and are published in [14]. Therefore we can test the quality of the approximation for F_2 and assume that it also works for g_1 using the same values for Q^2. Since we already have the exact form of the coefficient functions $L_q^{\mathrm{NS},(2)}$ corresponding to the Compton process in (2.17) there is no need for an approximation here. The same holds for the Born approximation given by $H_g^{(1)}$ in (2.14).

In the case of the bremsstrahlung reaction (2.16) and the Bethe-Heitler process (2.17), which lead to the heavy quark coefficient functions $H_g^{(2)}$ and $H_q^{(2)}$ respectively, we propose the following approximation

$$H_g^{(2),\mathrm{approx}}\Big(z,\xi,\frac{m^2}{\mu^2}\Big) = \Big(1-\frac{4m^2}{s}\Big)^{1/2} H_g^{(2)}\Big(z,\xi,\frac{m^2}{\mu^2}\Big) + \Big(\frac{4m^2}{s}\Big)^{1/4} H_g^{(1)}\Big(z,\xi\Big) S_{\mathrm{thres}}(s,m^2) \tag{5.1}$$

with

$$S_{\rm thres}(s,m^2) = C_A\Big[4\ln^2\Big(1-\frac{4m^2}{s}\Big) - 20\ln\Big(1-\frac{4m^2}{s}\Big) \\ +4\ln\frac{m^2}{\mu^2}\ln\Big(1-\frac{4m^2}{s}\Big)\Big] \\ +\Big(C_F-\frac{C_A}{2}\Big)\frac{2\pi^2}{\sqrt{1-4m^2/s}} \tag{5.2}$$

and

$$H_q^{(2),\rm approx}\Big(z,\xi,\frac{m^2}{\mu^2}\Big) = \Big(1-\frac{4m^2}{s}\Big)^{1/2} H_q^{(2)}\Big(z,\xi,\frac{m^2}{\mu^2}\Big)\,, \tag{5.3}$$

where ξ and z are defined in (2.15) and s is the virtual photon-parton CM energy. Expressed in z and ξ the latter becomes equal to

$$s = \Big(\frac{1-z}{z}\Big)\xi m^2\,. \tag{5.4}$$

The spin dependent heavy quark coefficient functions on the right hand side of (5.1), (5.3) are given in appendix B and they are strictly valid for $\xi = Q^2/m^2 \gg 1$. To improve their behaviour near threshold ($s = 4m^2$) we multiply them by the factor $(1-4m^2/s)^{1/2}$. Further we add to (5.1) a term which is obtained by multiplying the exact Born coefficient function $H_g^{(1)}$ (2.14) by the factor $S_{\rm thres}$ (5.2). The logarithmic terms in this factor originate from soft gluon bremsstrahlung which is the dominant production mechanism near the threshold in process (2.16) (see [16], [17]). The last term in (5.2) represents the Coulomb singularity which can be attributed to the loop-graphs where one gluon is exchanged between the massive quark antiquark pair. The factor $S_{\rm thres}$ is universal (see [17]) and is the same for F_2 and g_1. It has been computed for F_2 in eq. (5.7) of [14]. To suppress unwanted effects at larger s we have removed the factor 8 in the argument of the logarithms in eq. (5.7) of [14] and multiplied $S_{\rm thres}$ with $(4m^2/s)^{1/4}$ so that the second part in (5.1) vanishes when $s \gg m^2$.

To test the approximation made above we apply it first to $F_2(x,Q^2,m^2)$ for which the exact [14] as well as the asymptotic coefficient functions $H_{2,l}^{(2)}$ ($l = q,g$), valid for $Q^2 \gg m^2$, (see appendix D in [15]) are known. To that

purpose we plot the ratio

$$R(x,Q^2,m^2)=\frac{F_2^{\rm approx}(x,Q^2,m^2)}{F_2^{\rm exact}(x,Q^2,m^2)} \tag{5.5}$$

in NLO and examine below for which ξ (or Q^2) this approximation breaks down. Here F_2 is given by the same formula as in eq. (2.9) where now the heavy quark coefficient functions stand for the spin averaged ones. In eq. (5.4) the superscripts 'exact' and 'approx' indicate whether the exact heavy quark coefficients in [14] are used or the spin averaged analogues of the approximations in (5.1), (5.3). Notice that for the Born coefficient functions the exact formula has been taken.

For our plots of R in (5.5) we have chosen the parton density set GRV in the $\overline{\rm MS}$-scheme [30]. Further we limit ourselves to charm production ($m_c = m = 1.5$ GeV/c^2) which implies that the number of light flavours n_f in (2.9) has to be taken to be three in the coefficient functions and the running coupling constant $\alpha_s(\mu^2)$ ($\Lambda^{(3)}_{\overline{\rm MS}} = 248$ MeV). The factorization/renormalization scale μ^2 is set equal to Q^2. We have studied $R(x,Q^2,m^2)$ in the range $10^{-4} < x < 1$ and $10 < Q^2 < 10^4$ (GeV/c)^2.

In fig. 5 we have plotted R (5.5) as a function of Q^2 at $x = 0.1, 0.01, 10^{-3}$ and 10^{-4}. From this figure one infers that for $Q^2 > Q^2_{\rm min} > 20$ (GeV/c)^2 R is very close to one (actually $0.9 < R < 1.1$) which means that above this value $F_2^{\rm exact}$ and $F_2^{\rm approx}$ coincide. Even for $Q^2 > 10$ (GeV/c)^2 the approximation is rather good if one bears in mind that the statistics of deep inelastic charm production is quite low. For $x > 0.1$ the approximation gets worse which is revealed by fig. 6. Here $R > 1.2$ which happens for $x = 0.2$ when $Q^2 = 10$ (GeV/c)^2 or $x > 0.5$ when $Q^2 = 100$ (GeV/c)^2. Therefore we can conclude that the approximation breaks down at large x and small Q^2-values. In the case of the HERA collider this is not bad because the large x-regime is not accessible. However for fixed target experiments where x is large and Q^2 is small our predictions of the NLO corrections have to be considered as an order-of-magnitude estimate only.

Next we study the validity of our approximation for the charm component of the spin structure function denoted by $g_1(x,Q^2,m^2)$ (2.9). Here we choose the leading log (LL) parametrization and the next-to-leading log (NLL) parametrization in the $\overline{\rm MS}$-scheme for the spin parton densities in [31]. Here one has two sets of parton densities which are obtained in the standard scenario and the valence scenario. Our subsequent plots are made

in the standard scenario although we also studied the valence one. It turns out that the differences between both scenarios are irrelevant for charm production so that we do not present separate figures for the valence scenario. Further the number of flavours and the running coupling constant are the same as those taken for $F_2(x,Q^2,m^2)$ above. Since the exact coefficient functions $H_l^{(2),\mathrm{exact}}$ $(l=q,g)$ are unknown a comparison between the exact and approximate spin structure function g_1 can be only made on the Born level. Furthermore g_1 is not a positive definite quantity either in the exact or approximate formulae. This implies that the numerator and the denominator in (5.5) can vanish so that it makes no sense to plot R in the polarized case. Therefore we have to study the approximation on the level of the structure function itself.

In figs. 7a,7b and 7c we have plotted g_1^{exact} and g_1^{approx} on the Born level for $Q^2 = 10, 50$ and 100 $(\mathrm{GeV}/c)^2$ respectively. Here g_1^{approx} is obtained from the asymptotic coefficient function in (B.1) by multiplying the latter with $(1-4m^2/s)^{1/2}$. At $Q^2 = 10$ $(\mathrm{GeV}/c)^2$ (fig. 7a) the deviation between the exact and approximated result is of the order of 25% for $x < 0.02$. For larger x-values the approximation becomes much better. When Q^2 increases (see figs. 7b,7c) g_1^{exact} (Born) and g_1^{approx}(Born) almost coincide over the whole x-region. In NLO we have to take the approximate order α_s correction to the charm structure function $g_1(x,Q^2,m^2)$ because not all exact order α_s^2 heavy quark coefficient functions are known. Denoting this approximation by g_1^{approx}(NLO) we assume that its validity holds for the same x and Q^2-values as those observed for F_2^{approx} above i.e. $x < 0.1$ and $Q^2 \gg 10$ $(\mathrm{GeV}/c)^2$. For $x > 0.1$ we expect that the exact NLO charm structure function will be very small which is already indicated by the Born contribution in figs. 7a,7b and 7c. The expression for g_1^{approx}(NLO) is obtained by adding to g_1^{exact}(Born) the order α_s corrections. The latter originate from the exact expression for $L_q^{\mathrm{NS},(2)}$ (2.18) and $H_l^{(2),\mathrm{approx}}$ $(l=q,g)$ given in (5.1), (5.3). The results for g_1^{approx} up to NLO are presented in figs. 8a, 8b and 8c for $Q^2 = 10, 50$ and 100 $(\mathrm{GeV}/c)^2$ respectively, where they are compared with the Born contribution. From these figures we infer that the bulk of the correction occurs in the region $0.01 < x < 0.1$ and amounts to almost 100% ($g_1^{\mathrm{approx}}/g_1^{\mathrm{exact}}(\mathrm{Born}) \sim 2$).

In figs. 9a, 9b and 9c we have plotted in NLO $g_1^{\mathrm{approx}}(x,Q^2,m^2)$ and $g_1^{\mathrm{light}}(x,Q^2)$ where the latter structure function is due to light partons (u,d,s and g) only. Below $x = 2\times 10^{-3}$ the charm as well as the light parton

contribution can become negative so that in this region we have taken the absolute values of g_1. Further we observe that the charm component of the total structure function $g_1^{\rm light}+g_1^{\rm approx}$ is small. At $Q^2 = 10$ (GeV/c)^2 (fig. 9a) it becomes maximal at $x = 10^{-3}$ where it amounts to 14% of the light parton contribution. At larger Q^2-values i.e. $Q^2 = 50, 100$ (GeV/c)^2 (see figs. 9b,9c) the maximum occurs at $x = 0.01$ where it is only 4%. From these results we conclude that the charm component of the structure function g_1 is much smaller than the one discovered for F_2 in [14]. In the latter case it becomes as large as 40% in the small x-region ($x = 10^{-4}$). The above predictions made for $g_1(x, Q^2, m^2)$ up to NLO can be considered as reliable because the bulk of the corrections are in the region $x < 0.1$ at Q^2-values for which $F_2^{\rm approx}$ and $g_1^{\rm approx}$ (Born) are close to their exact values. This region is accessible to fixed target and HERA experiments where in the latter case both the electron beam and proton beam are polarized.

Summarizing our work we have computed the order α_s^2 contributions to the heavy quark coefficient functions corresponding to the spin structure function $g_1(x, Q^2, m^2)$. For the Compton process (2.17) we were able to calculate the exact coefficient function $L_q^{\rm NS,(2)}$. In the case of the photon-gluon fusion process (2.16) and the Bethe-Heitler process (2.17) we could only obtain an analytic expression of $H_l^{(2)}$ ($l = q, g$) in the asymptotic regime $Q^2 \gg m^2$. The last expressions will serve as a check on the exact coefficient functions which can be computed in a semi-analytic way similar to the procedure outlined in [14]. To estimate the NLO corrections to $g_1(x, Q^2, m^2)$ we modified the asymptotic coefficient functions according to (5.1), (5.3) in order to mimic the exact form. This approximation was tested for F_2 and g_1 (Born) and lead to reasonable results as long as $Q^2 > 10$ (GeV/c)^2 and $x < 0.1$. Using this approximation we found that the order α_s corections to $g_1(x, Q^2, m^2)$ are large but the charm component of the total spin structure function given by $g_1^{\rm light} + g_1^{\rm approx}$ is small.

Appendix A

Here we present the unrenormalized spin dependent operator matrix elements $\hat{A}_{ij}^{(2)}$ whose general structure was expressed in renormalization group coefficients in section 3. After having carried out mass renormalization the two-loop OME is given by the following expression (see also (3.22))

$$\begin{aligned}
\hat{A}_{Qg}^{(2)}\Big(\frac{m^2}{\mu^2},\epsilon\Big) &= S_\epsilon^2\Big(\frac{m^2}{\mu^2}\Big)^\epsilon\Big[\frac{1}{\epsilon^2}\Big\{C_F T_f\Big[(16-32z)[\ln z - 2\ln(1-z)] + 24\Big] \\
&+C_A T_f[(32-64z)\ln(1-z) - 64(1+z)\ln z - 192(1-z)]\Big\} \\
&+\frac{1}{\epsilon}\Big\{C_F T_f\Big[(4-8z)[2\ln^2(1-z) + \ln^2 z - 4\ln z\ln(1-z) - 4\zeta(2)] \\
&-32(1-z)\ln(1-z) + (4-64z)\ln z - 8 - 12z\Big] \\
&+C_A T_f\Big[(8+16z)[2\mathrm{Li}_2(-z) + 2\ln z\ln(1+z) + \ln^2 z] \\
&-(8-16z)\ln^2(1-z) + 16\zeta(2) + 32(1-z)\ln(1-z) \\
&-(8+64z)\ln z - 96 + 88z\Big]\Big\} + a_{Qg}^{(2)}(z)\Big] \\
&+\sum_{H=Q}^{t} S_\epsilon^2\Big(\frac{m_H^2}{\mu^2}\Big)^{\epsilon/2}\Big(\frac{m^2}{\mu^2}\Big)^{\epsilon/2}\Big[\frac{1}{\epsilon^2}T_f^2\Big(\frac{64}{3} - \frac{128}{3}z\Big) \\
&\quad\times\Big(1 + \frac{\epsilon^2}{4}\zeta(2)\Big)\Big], \qquad\qquad (A.1)
\end{aligned}$$

with

$$\begin{aligned}
a_{Qg}^{(2)}(z) &= C_F T_f\Big\{(-1+2z)[8\zeta(3) + 8\zeta(2)\ln(1-z) + \frac{4}{3}\ln^3(1-z) \\
&-8\ln(1-z)\mathrm{Li}_2(1-z) + 4\zeta(2)\ln z - 4\ln z\ln^2(1-z) \\
&+\frac{2}{3}\ln^3 z - 8\ln z\mathrm{Li}_2(1-z) + 8\mathrm{Li}_3(1-z) - 24\mathrm{S}_{1,2}(1-z)] \\
&-(116 - 48z - 16z^2)\mathrm{Li}_2(1-z) + (50 - 32z - 8z^2)\zeta(2) \\
&-(72 - 16z - 8z^2)\ln z\ln(1-z) + (12 - 8z - 4z^2)\ln^2(1-z) \\
&-(5 - 8z - 4z^2)\ln^2 z - (64 - 60z)\ln(1-z) \\
&-(16 + 50z)\ln z - 22 + 46z\Big\} \\
&+C_A T_f\Big\{(-1+2z)[-8\zeta(2)\ln(1-z) - \frac{4}{3}\ln^3(1-z)
\end{aligned}$$

$$
\begin{aligned}
&+8\ln(1-z)\mathrm{Li}_2(1-z) - 8\mathrm{Li}_3(1-z)] + (1+2z)\Big[- \frac{4}{3}\ln^3 z \\
&-8\zeta(2)\ln(1+z) - 16\ln(1+z)\mathrm{Li}_2(-z) - 8\ln z\ln^2(1+z) \\
&+4\ln^2 z\ln(1+z) + 8\ln z\mathrm{Li}_2(-z) - 8\mathrm{Li}_3(-z) - 16\mathrm{S}_{1,2}(-z)\Big] \\
&+16(1+z)[4\mathrm{S}_{1,2}(1-z) + 2\ln z\mathrm{Li}_2(1-z) - 3\zeta(2)\ln z + \mathrm{Li}_2(-z) \\
&+\ln z\ln(1+z)] - 16(1-z)\zeta(3) + (100 - 112z - 8z^2)\mathrm{Li}_2(1-z) \\
&-(132 - 144z - 4z^2)\zeta(2) - 4z(4+z)\ln z\ln(1-z) \\
&-(10 - 8z - 2z^2)\ln^2(1-z) - (6+2z^2)\ln^2 z \\
&+4\ln(1-z) - (56+148z)\ln z - 204 + 212z\Big\}\,. \qquad \text{(A.2)}
\end{aligned}
$$

The unrenormalized OME corresponding to fig. 3 (see (3.28)) is given by

$$
\begin{aligned}
&\hat{A}_{Qq}^{\mathrm{PS},(2)}\Big(\frac{m^2}{\mu^2},\epsilon\Big) = S_\epsilon^2\Big(\frac{m^2}{\mu^2}\Big)^\epsilon C_F T_f\Big\{\frac{1}{\epsilon^2}\Big(- 32(1+z)\ln z - 80(1-z)\Big) \\
&+\frac{1}{\epsilon}\Big(8(1+z)\ln^2 z + 8(1-3z)\ln z - 8(1-z)\Big) + a_{Qq}^{\mathrm{PS},(2)}(z)\Big\}\,, \qquad \text{(A.3)}
\end{aligned}
$$

with

$$
\begin{aligned}
a_{Qq}^{\mathrm{PS},(2)}(z) &= (1+z)[32\mathrm{S}_{1,2}(1-z) + 16\ln z\mathrm{Li}_2(1-z) - 24\zeta(2)\ln z \\
&-\frac{4}{3}\ln^3 z] + 20(1-z)[2\mathrm{Li}_2(1-z) - 3\zeta(2)] - (2-6z)\ln^2 z \\
&-(12+60z)\ln z - 72(1-z)\,. \qquad \text{(A.4)}
\end{aligned}
$$

Appendix B

In this appendix we present the spin dependent heavy quark coefficient functions $H_i^{(2)}$ and $L_i^{(2)}$ $(i = q, g)$ in the asymptotic limit $Q^2 \gg m^2$. Starting with the lowest order photon-gluon fusion process (2.13) the heavy quark coefficient function reads (see (4.3))

$$H_g^{(1)}\Big(z, \frac{Q^2}{m^2}, \frac{m^2}{\mu^2}\Big) = T_f[-4(1-2z)\Big(\ln\frac{Q^2}{m^2} + \ln(1-z) - \ln z\Big) + 4(3-4z)]\,. \tag{B.1}$$

In next-to-leading order the coefficient function corresponding to the virtual corrections to the Born reaction (2.13) and the bremstrahlung process (2.16) are given by (see (4.6))

$$\begin{aligned}
H_g^{(2)}\Big(z, \frac{Q^2}{m^2}, \frac{m^2}{\mu^2}\Big) = {} & \Big[C_F T_f\{(8z-4)(2\ln(1-z) - \ln z) + 6\} \\
& + C_A T_f\{-8(1-2z)\ln(1-z) + 16(1+z)\ln z + 48(1-z)\}\Big]\ln^2\frac{Q^2}{m^2} \\
& + \Big[C_F T_f\{-8(1-2z)[\mathrm{Li}_2(1-z) - 3\ln z\ln(1-z) \\
& + 2\ln^2(1-z) + \ln^2 z - 4\zeta(2)] \\
& + 4(17-20z)\ln(1-z) - 16(3-2z)\ln z - 4(17-13z)\} \\
& + C_A T_f\{-16(1+2z)[\mathrm{Li}_2(-z) + \ln z\ln(1+z)] \\
& + 32(1+z)\mathrm{Li}_2(1-z) + 48\ln z\ln(1-z) - 8(1-2z)\ln^2(1-z) \\
& - 8(3+4z)\ln^2 z - 32z\zeta(2) + 16(7-8z)\ln(1-z) \\
& - 24(5-4z)\ln z - 8(20-21z)\}\Big]\ln\frac{Q^2}{m^2} \\
& + C_A T_f\Big[\{-16(1-2z)\ln(1-z) + 32(1+z)\ln z + 96(1-z)\}\ln\frac{Q^2}{m^2} \\
& + 32(1+z)\mathrm{Li}_2(1-z) + 48\ln z\ln(1-z) - 16(1-2z)\ln^2(1-z) \\
& - 16(1+z)\ln^2 z + 16(9-10z)\ln(1-z) \\
& - 32(4-z)\ln z + 16(1-2z)\zeta(2) - 256(1-z)\Big]\ln\frac{m^2}{\mu^2} \\
& + C_F T_f\Big[(1-2z)[24\mathrm{Li}_3(1-z) - 8\ln(1-z)\mathrm{Li}_2(1-z)
\end{aligned}$$

$$
\begin{aligned}
&-32\zeta(2)\ln z - 8\ln^3(1-z) + 20\ln z\ln^2(1-z)\\
&-16\ln^2 z\ln(1-z) + \frac{8}{3}\ln^3 z]\\
&-16(1+z)^2[4\mathrm{S}_{1,2}(-z) + 4\ln(1+z)\mathrm{Li}_2(-z)\\
&+2\ln z\ln^2(1+z) - \ln^2 z\ln(1+z) + 2\zeta(2)\ln(1+z)]\\
&-(32-192z+32z^2)\mathrm{Li}_3(-z) - (96-16z^2)\mathrm{Li}_2(1-z)\\
&+32(1-z)^2[\mathrm{S}_{1,2}(1-z) + \ln z\mathrm{Li}_2(-z)]\\
&+(\frac{64}{3z} + 64z + \frac{208}{3}z^2)[\mathrm{Li}_2(-z) + \ln z\ln(1+z)]\\
&+(66-80z-4z^2)\ln^2(1-z) - 32z^2\zeta(2)\ln(1-z)\\
&-(188-164z-16z^2)\ln(1-z) + (36-8z-\frac{92}{3}z^2)\ln^2 z\\
&-(160-112z-8z^2)\ln z\ln(1-z) + \frac{1}{3}(320-424z-48z^2)\ln z\\
&-(48-224z-32z^2)\zeta(3) - \frac{1}{3}(192-336z-184z^2)\zeta(2)\\
&+\frac{1}{3}(304-244z)\Big]\\
&+C_A T_f\Big[16(1+2z)\Big(\mathrm{Li}_3\Big(\frac{1-z}{1+z}\Big) - \mathrm{Li}_3\Big(-\frac{1-z}{1+z}\Big)\\
&-\ln(1-z)\mathrm{Li}_2(-z) - \ln z\ln(1-z)\ln(1+z)\Big)\\
&+8(1+2z+2z^2)[2\mathrm{S}_{1,2}(-z) + \ln z\ln^2(1+z)\\
&+2\ln(1+z)\mathrm{Li}_2(-z) + \zeta(2)\ln(1+z)]\\
&+(72+80z-16z^2)\mathrm{S}_{1,2}(1-z) - 16(2+z)[2\mathrm{Li}_3(1-z)\\
&+\ln^2 z\ln(1-z)] - (12+24z-8z^2)[2\mathrm{Li}_3(-z)\\
&-\ln^2 z\ln(1+z) - 2\ln z\mathrm{Li}_2(-z)]\\
&-\frac{16}{3}\Big(\frac{2}{z} + 3 + 9z + 11z^2\Big)[\mathrm{Li}_2(-z) + \ln z\ln(1+z)]\\
&+24\ln z\ln^2(1-z) + 16\ln z\mathrm{Li}_2(1-z)\\
&+32(1+z)\ln(1-z)\mathrm{Li}_2(1-z) + (76-112z-8z^2)\mathrm{Li}_2(1-z)\\
&+(38-48z+2z^2)\ln^2(1-z) + (24-80z+16z^2)\zeta(2)\ln(1-z)\\
&+\frac{8}{3}(3+4z)\ln^3 z + \Big(84-32z+\frac{82}{3}z^2\Big)\ln^2 z\\
&-(136-112z+4z^2)\ln z\ln(1-z) - (80+32z)\zeta(2)\ln z
\end{aligned}
$$

$$+\frac{1}{3}(776-652z+24z^2)\ln z-(172-212z+8z^2)\ln(1-z)$$
$$-(28+24z+16z^2)\zeta(3)-\Big(228-224z+\frac{164}{3}z^2\Big)\zeta(2)$$
$$+\frac{1}{3}(808-832z)\Big]. \tag{B.2}$$

The coefficient function corresponding to the Bethe-Heitler process (2.17) reads (see (4.9))

$$\begin{aligned}
H_q^{(2)}\Big(z,\frac{Q^2}{m^2},\frac{m^2}{\mu^2}\Big) &= C_F T_f\Big[\Big\{8(1+z)\ln z+20(1-z)\Big\}\ln^2\frac{Q^2}{m^2}\\
&+\Big\{[16(1+z)\ln z+40(1-z)]\ln\frac{Q^2}{m^2}\\
&+8(1+z)[2\mathrm{Li}_2(1-z)+2\ln z\ln(1-z)-\ln^2 z]+40(1-z)\\
&\times\ln(1-z)-(56-8z)\ln z-96(1-z)\Big\}\ln\frac{m^2}{\mu^2}\\
&+\{16(1+z)[\mathrm{Li}_2(1-z)+\ln z\ln(1-z)-\ln^2 z]\\
&+40(1-z)\ln(1-z)-32(2-z)\ln z-88(1-z)\}\ln\frac{Q^2}{m^2}\\
&+(1+z)\Big(32\,\mathrm{S}_{1,2}(1-z)-16\mathrm{Li}_3(1-z)+8\ln z\ln^2(1-z)\\
&-16\ln^2 z\ln(1-z)+16\ln(1-z)\mathrm{Li}_2(1-z)-32\zeta(2)\ln z\\
&+\frac{16}{3}\ln^3 z\Big)+16(1-3z)\mathrm{Li}_2(1-z)\\
&-\Big(\frac{32}{3z}+32+32z+\frac{32}{3}z^2\Big)[\mathrm{Li}_2(-z)+\ln z\ln(1+z)]\\
&-\Big(112-80z+\frac{32}{3}z^2\Big)\zeta(2)-32(2-z)\ln z\ln(1-z)\\
&+(1-z)\Big(20\ln^2(1-z)-88\ln(1-z)+\frac{592}{3}\Big)\\
&+\Big(56+\frac{16}{3}z^2\Big)\ln^2 z+\frac{256}{3}\Big(2-z\Big)\ln z\Big]. \qquad \text{(B.3)}
\end{aligned}$$

Finally we present the coefficient function originating from the Compton process (2.17). The asymptotic form is given by (4.12) and can be analytically expressed as

$$
\begin{aligned}
L_q^{\mathrm{NS},(2)}\Big(z,\frac{Q^2}{m^2},\frac{m^2}{\mu^2}\Big) &= C_F T_f\Big[\frac{4}{3}\left(\frac{1+z^2}{1-z}\right)\ln^2\frac{Q^2}{m^2}+\Big\{\frac{1+z^2}{1-z}\Big(\frac{8}{3}\ln(1-z)\\
&-\frac{16}{3}\ln z-\frac{58}{9}\Big)-2+6z\Big\}\ln\frac{Q^2}{m^2}\\
&+\Big(\frac{1+z^2}{1-z}\Big)\Big(-\frac{8}{3}\mathrm{Li}_2(1-z)-\frac{8}{3}\zeta(2)-\frac{16}{3}\ln z\ln(1-z)\\
&+\frac{4}{3}\ln^2(1-z)+4\ln^2 z-\frac{58}{9}\ln(1-z)+\frac{134}{9}\ln z+\frac{359}{27}\Big)\\
&-\Big(2-6z\Big)\ln(1-z)+\Big(\frac{10}{3}-10z\Big)\ln z+\frac{19}{3}-19z\Big]\,. \qquad \text{(B.4)}
\end{aligned}
$$

In the above expression one should bear in mind that the singularity at $z = 1$ will never show up because of the kinematical constraint $z < Q^2/(Q^2+4m^2)$. However after convoluting $L_q^{\mathrm{NS},(2)}$ by the parton densities, the structure function $g_1(x,Q^2,m^2)$ will diverge as $\ln^3(Q^2/m^2)$ in the limit $Q^2 \gg m^2$. In this limit the upper boundary $z_{\max}$ in (2.9) will tend to one and the virtual gluon which decays into the heavy quark pair becomes soft. The soft gluon annihilation which causes the cubic logarithm above has to be added to the two-loop vertex correction containing the heavy quark (Q) loop which is calculated in appendix A of [32]. In this way the cubic logarithm is then cancelled. The final result will be that in (B.4) the singular terms at $z = 1$ have to be replaced by the distributions $(\ln^k(1-z)/(1-z))_+$ defined by

$$
\int_0^1 dz\,\Big(\frac{\ln^k(1-z)}{1-z}\Big)_+ f(z) = \int_0^1 dz\,\Big(\frac{\ln^k(1-z)}{1-z}\Big)\{f(z)-f(1)\}\,, \qquad \text{(B.5)}
$$

and one has to add the following delta function contribution to (B.4)

$$
\begin{aligned}
L_q^{\mathrm{NS,S+V},(2)}\Big(z,\frac{Q^2}{m^2},\frac{m^2}{\mu^2}\Big) &= C_F T_f\delta(1-z)\Big\{2\ln^2\Big(\frac{Q^2}{m^2}\Big)-\Big[\frac{32}{3}\zeta(2)+\frac{38}{3}\Big]\\
&\times\ln\Big(\frac{Q^2}{m^2}\Big)+\frac{268}{9}\zeta(2)+\frac{265}{9}\Big\}\,. \qquad \text{(B.6)}
\end{aligned}
$$

References

[1] A. Ali et. al. "Heavy Quarks" in Proceedings of the Workshop "Physics at HERA", October 29-30 1991, Hamburg, Germany. Eds. W. Buchmüller and G. Ingelman, p.667.

[2] A. Vogt, DESY-96-012.

[3] C. Adloff et al., (H1 Collaboration) DESY96-138.

[4] ZEUS Collaboration, XXVIII International Conference on High Energy Physics, Warsaw, (1996).

[5] E. Witten, Nucl. Phys. **B104** (1976) 445;
J. Babcock and D. Sivers, Phys. Rev. **D18** (1978) 2301;
M. A. Shifman, A.I. Vainstein and V.J. Zakharov, Nucl. Phys. **B136** (1978) 157;
M. Glück and E. Reya, Phys. Lett. **B83** (1979) 98;
J. V. Leveille and T. Weiler, Nucl. Phys. **B147** (1979) 147.

[6] G. K. Mallot, Future semi-inclusive spin physics at CERN in "Workshop on the prospects of spin physics at HERA", 28-31 August 1995, Zeuthen, Germany, p.273.

[7] V. W. Hughes, Future HERA Experiment with 800 GeV polarized Protons, in "Workshop on Deep-Inelastic Scattering and QCD" 24-28 April 1995, Paris, France, p.515.

[8] J. Blümlein, On the Measurability of the structure function $g_1(x, Q^2)$ in ep collisions at HERA, in "Workshop on the prospects of spin physics at HERA". 28-31 August 1995, Zeuthen, Germany, p.179.

[9] S. Frixione and G. Ridolfi, GEF-TH-4/1996, ETH-TH/96-08, hep-ph/9605209.

[10] M. Stratmann and W. Vogelsang, DO-TH-96/10, RAL-TR-96-033, hep-ph/9605330.

[11] D. A. Walton, Z. Phys. **C12** (1982) 123.

[12] M. Glück, E. Reya and W. Vogelsang. Nucl. Phys. **B351** (1991) 579.

[13] W. Vogelsang, Z. Phys. **C50** (1991) 275.

[14] E. Laenen, S. Riemersma, J. Smith and W. L. van Neerven, Nucl. Phys. **B392** (1993) 162.

[15] M. Buza, Y. Matiounine, J. Smith, R. Migneron and W. L. van Neerven, Nucl. Phys. **B472** (1996) 611.

[16] R. Meng, G. A. Schuler, J. Smith, W. L. van Neerven, Nucl. Phys. **B339** (1990) 325.

[17] E. Laenen, J. Smith and W. L. van Neerven, Nucl. Phys. **B369** (1992) 543.

[18] S. Riemersma, J. Smith and W. L. van Neerven, Phys. Lett. **B347** (1995) 43. Some errors in the computer code used in this reference and in [3] are corrected in B. W. Harris and J. Smith, Nucl. Phys. **B452** (1995) 109.

[19] L. Lewin,"Polylogarithms and Associated Functions", North Holland, Amsterdam, 1983.
R. Barbieri, J.A. Mignaco and E. Remiddi, Nuovo Cimento **11A** (1972) 824.
A. Devoto and D.W. Duke, Riv. Nuovo. Cimento Vol. 7, N.6 (1984) 1.

[20] E. B. Zijlstra and W. L. van Neerven, Nucl. Phys. **B417** (1994) 61, Erratum **B426** (1994) 245;
E.B. Zijlstra , Ph.D. thesis , University of Leiden , 1993.

[21] R. Mertig and W. L. van Neerven, Z. Phys. **C70** (1996) 637.

[22] G. 't Hooft and M. Veltman, Nucl. Phys. **44** (1972) 189.

[23] P. Breitenlohner and B. Maison, Commun. Math. Phys. **53** 1977 11,39,55.

[24] D. Akyeampong and R. Delburgo, Nuovo Cimento **17A** (1973) 578; **18A** (1973) 94, **19A** (1974) 219.

[25] S. A. Larin, Phys. Lett. **B303** (1993) 113.

[26] J. A. M. Vermaseren, FORM2, published by Computer Algebra Netherlands (CAN), Kruislaan 413, 1098 SJ Amsterdam, The Netherlands.

[27] W. Vogelsang, Phys. Rev. **D54** (1996) 2023.

[28] G. Altarelli and G. Parisi, Nucl. Phys. **B126** (1977) 298.

[29] K. Sasaki, Prog. of Theor. Phys. **54** (1975) 1816.
M.A. Ahmed and G.G. Ross, Nucl. Phys. **B111** (1976) 441.

[30] M. Glück, E. Reya and A. Vogt, Z. Phys. **C67** (1995) 433.

[31] M. Glück, E. Reya, M. Stratmann and W. Vogelsang, Phys. Rev. **D53** (1996) 4775.

[32] P.J. Rijken and W.L. van Neerven, Phys. Rev. **D52** (1995) 149.

Figure Captions

Fig. 1. One-loop graphs contributing to the OME $A_{Qg}^{(1)}$. The solid line indicates the heavy quark Q.

Fig. 2. Two-loop graphs contributing to the OME $A_{Qg}^{(2)}$. The solid line indicates the heavy quark Q. Graphs $d.19$ and $d.20$ contain the external gluon self-energy with the heavy quark loop. In this loop a sum over all heavy quark species indicated by H ($m_H^2 \geq m^2$) is understood.

Fig. 3. Two-loop graphs contributing to the OME $A_{Qq}^{\mathrm{PS},(2)}$. The solid line represents the heavy quark Q whereas the dashed line stands for the light quark q.

Fig. 4. Two-loop graphs contributing to the OME $A_{qq,Q}^{\mathrm{NS},(2)}$. The gluon self-energy contains the heavy quark Q with mass m in the quark loop only which is indicated by the solid line. The dashed line stands for the light quark q.

Fig. 5. R (5.5) plotted as a function of Q^2 at fixed x; $x = 0.1$ (upper dotted line), $x = 0.01$ (solid line), $x = 10^{-3}$ (middle dotted line), $x = 10^{-4}$ (lower dotted line).

Fig. 6. R (5.5) plotted as a function of x at fixed Q^2; $Q^2 = 10$ (GeV/c)^2 (lower dotted line), $Q^2 = 50$ (GeV/c)^2 (middle line), $Q^2 = 100$ (GeV/c)^2 (solid line).

Fig. 7a. g_1^{exact} (Born) (dotted line) and g_1^{approx} (Born) (solid line) as a function of x for $Q^2 = 10$ (GeV/c)^2.

Fig. 7b. Same as in Fig. 7a but now for $Q^2 = 50$ (GeV/c)^2.

Fig. 7c. Same as in Fig. 7a but now for $Q^2 = 100$ (GeV/c)^2.

Fig. 8a. g_1^{exact} (Born) (dotted line) and g_1^{approx} (NLO) (solid line) as a function of x for $Q^2 = 10$ (GeV/c)^2.

Fig. 8b. Same as in Fig. 8a but now for $Q^2 = 50$ (GeV/c)^2.

Fig. 8c. Same as in Fig. 8a but now for $Q^2 = 100$ (GeV/c)^2.

Fig. 9a. $g_1^{\rm light}$ (solid line) and $g_1^{\rm approx}$ (dotted line) both in NLO as a function of x for $Q^2 = 10$ (GeV/c)^2. For $x < 10^{-3}$ both $g_1^{\rm light}$ and $g_1^{\rm approx}$ become negative so that we have taken their absolute values.

Fig. 9b. Same as in Fig. 9a but now for $Q^2 = 50$ (GeV/c)^2.

Fig. 9c. Same as in Fig. 9a but now for $Q^2 = 100$ (GeV/c)^2.

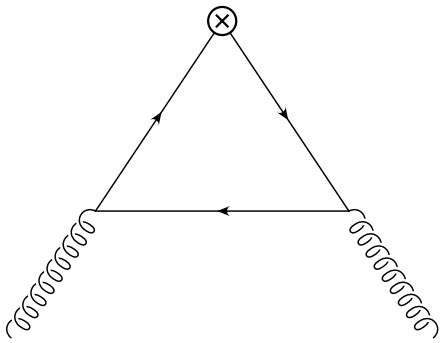

a

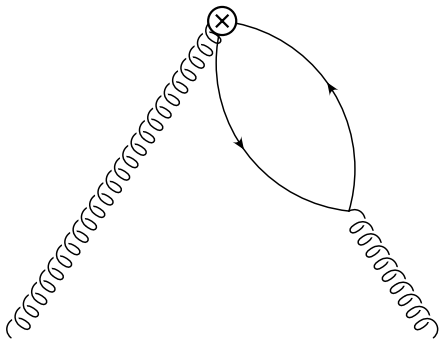

b

Fig. 1

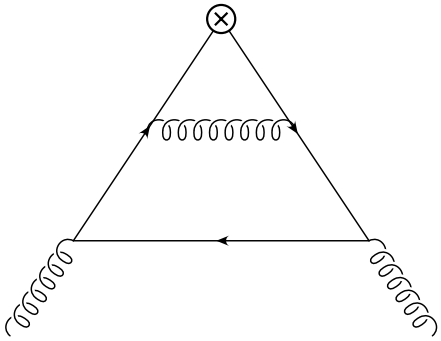

a

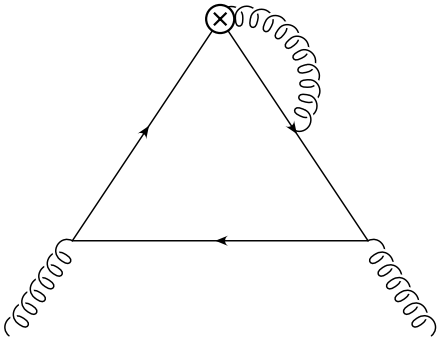

b

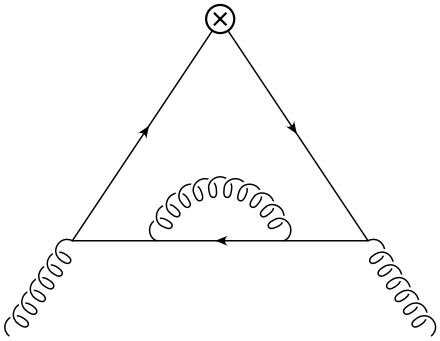

c

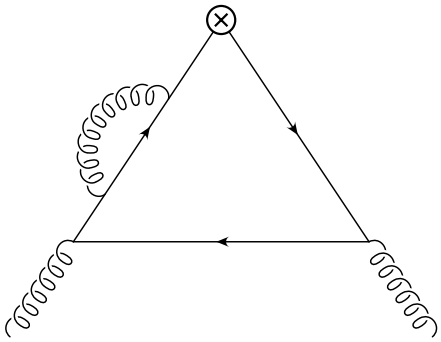

d

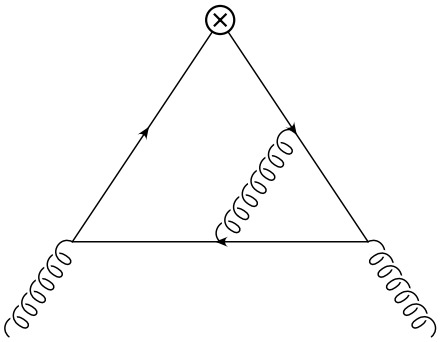

e

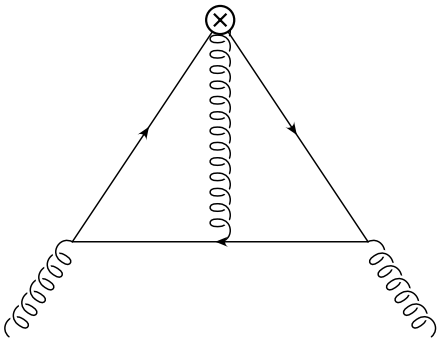

f

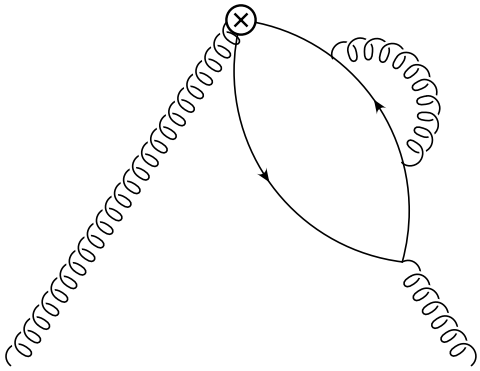

g

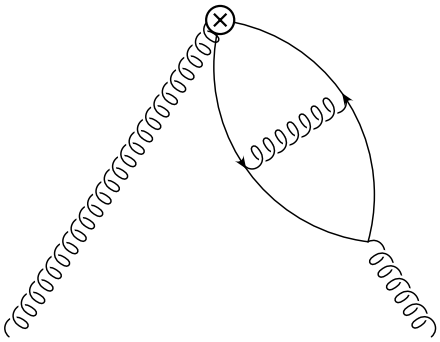

h

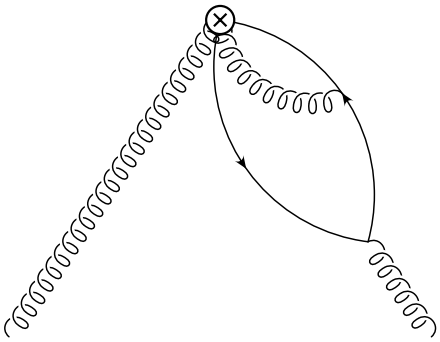

i

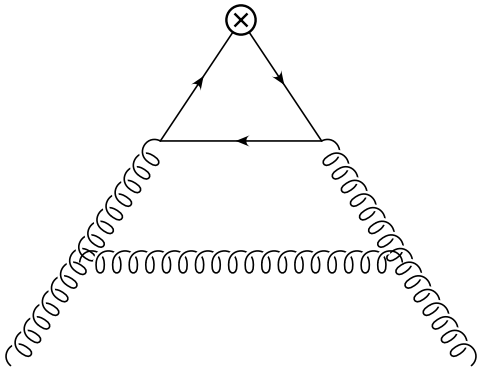

j

Fig. 2

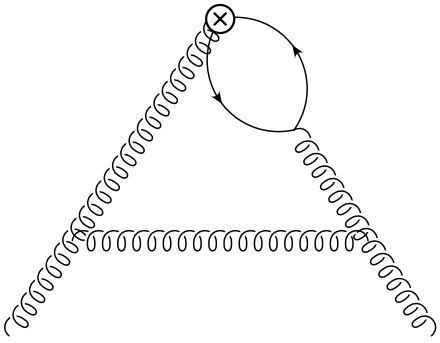

k

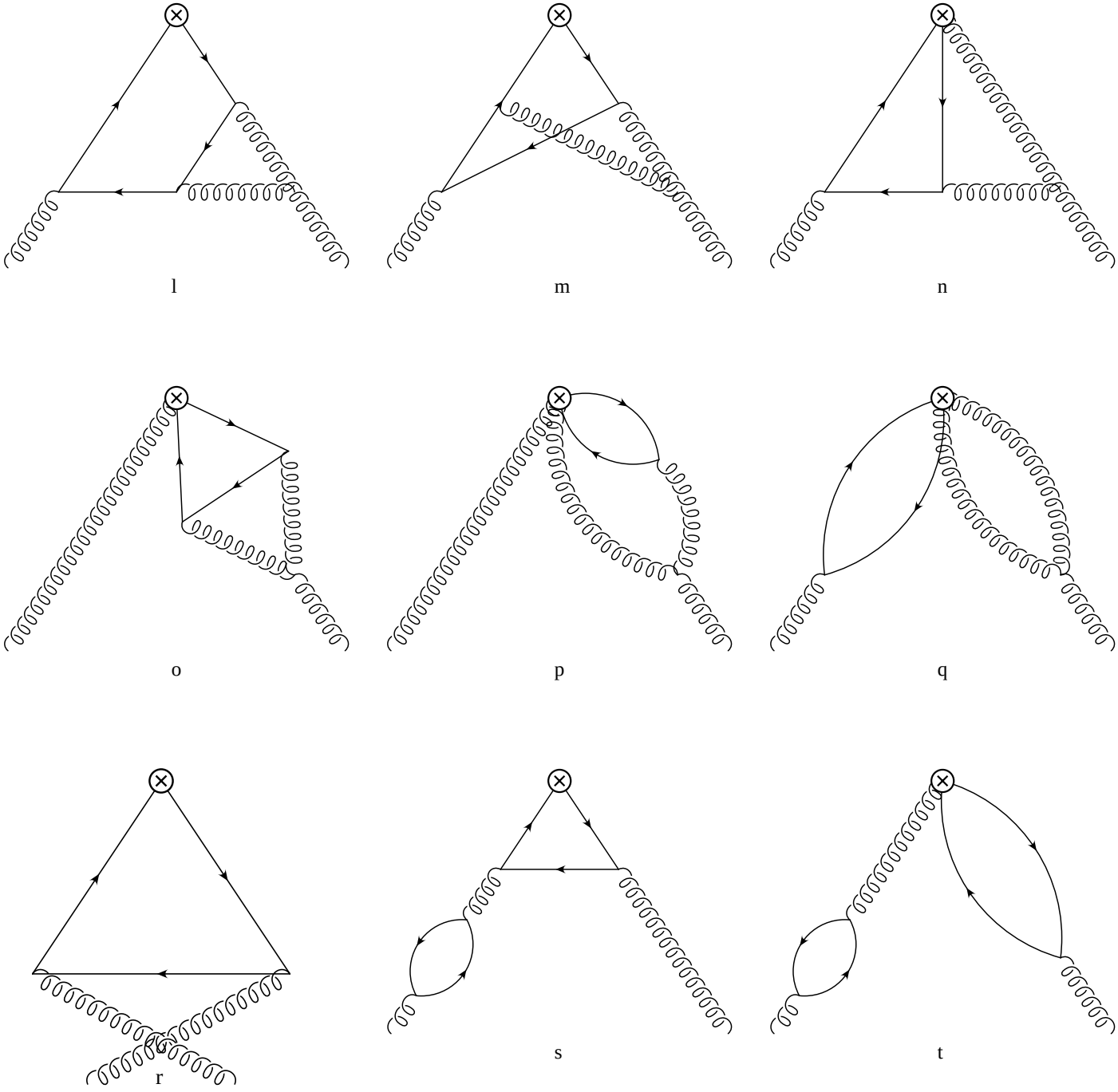

Fig. 2 (continued)

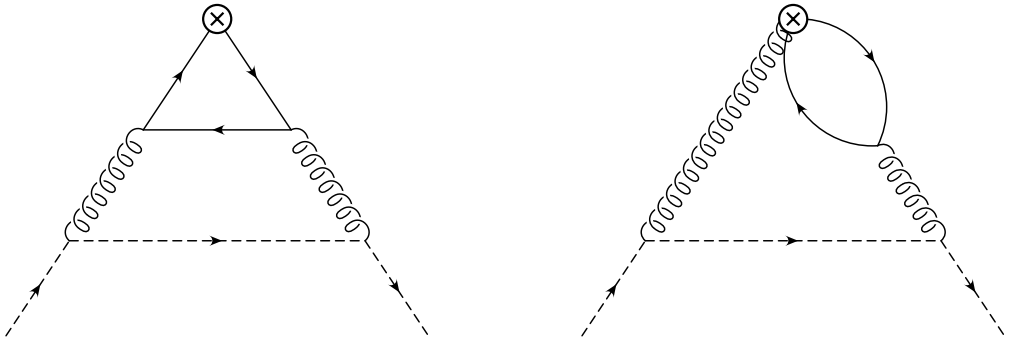

Fig. 3

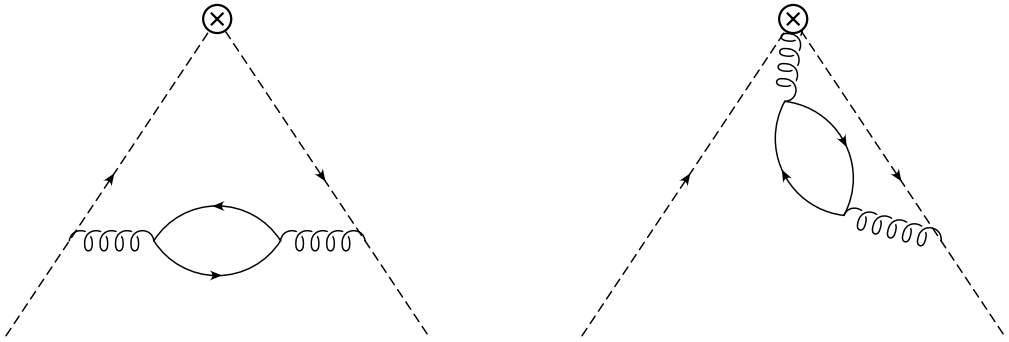

Fig. 4

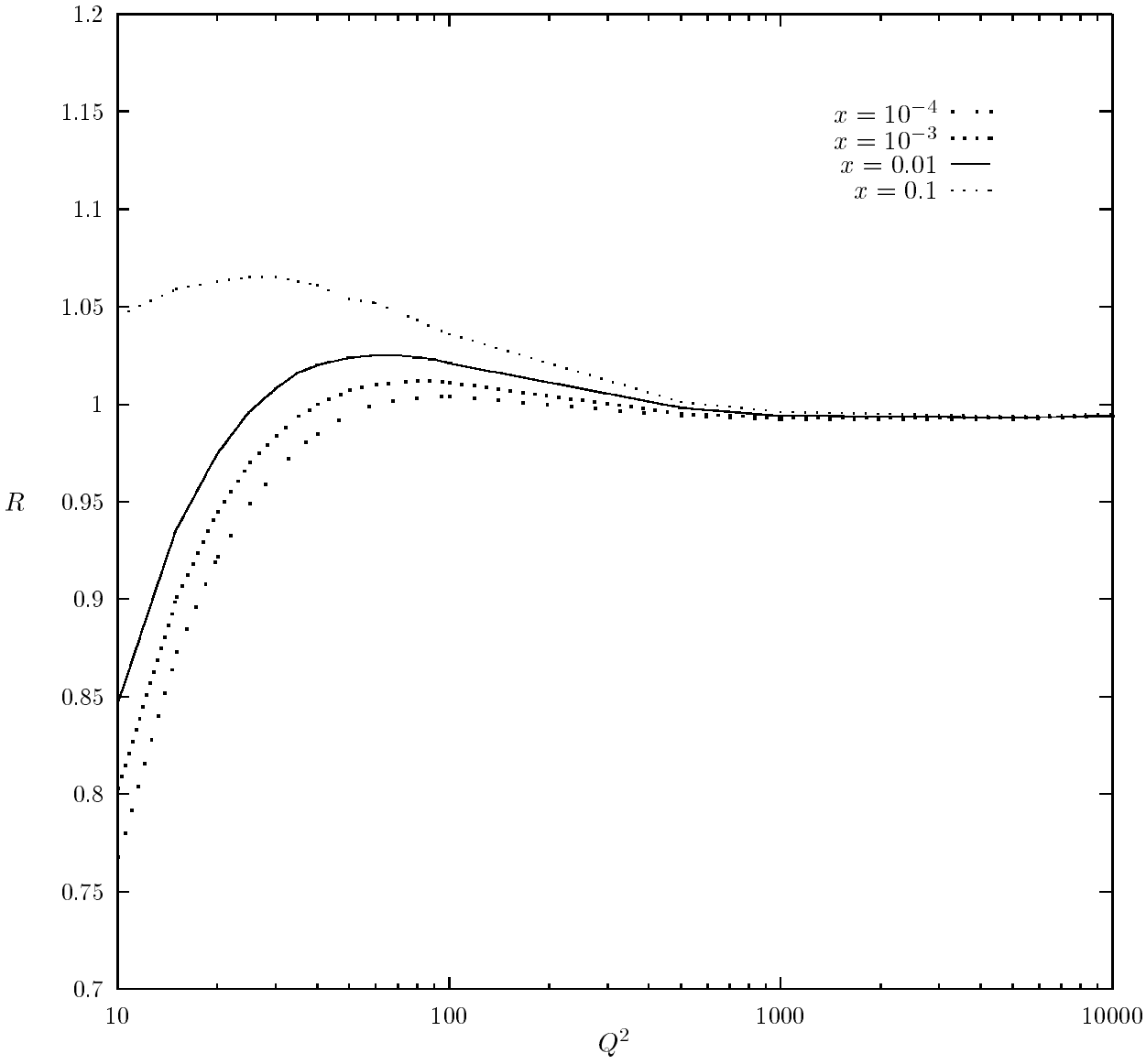
1.2
1.15
1.1
1.05
1
0.95
0.9
0.85
0.8
0.75
0.7
R
10
100
1000
10000
Q^2
$x = 10^{-4}$
$x = 10^{-3}$
$x = 0.01$
$x = 0.1$

Fig.5

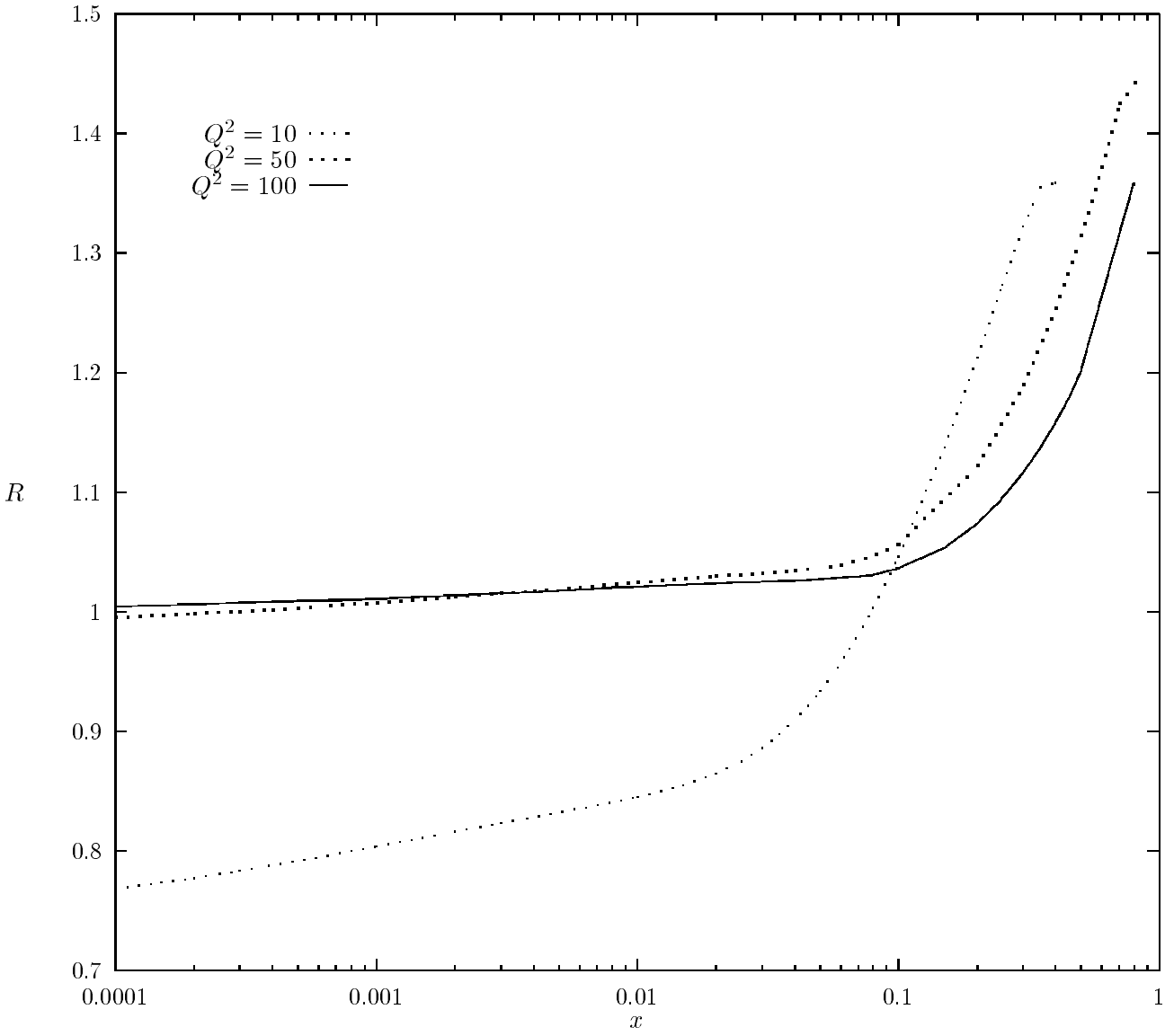

Fig.6

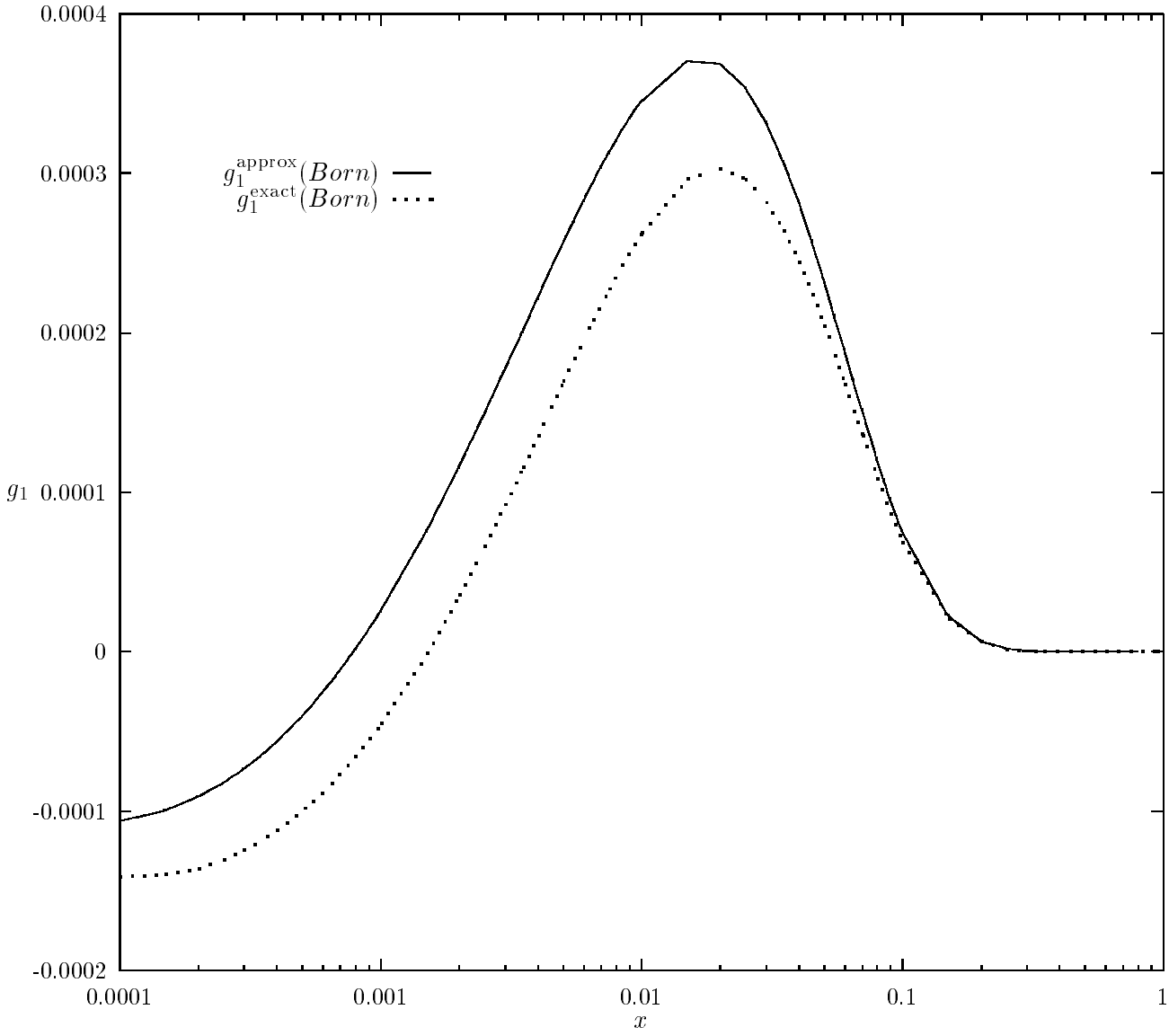
0.0004
0.0003
0.0002
0.0001
0
-0.0001
-0.0002
g_1
$g_1^{\rm approx}(Born)$
$g_1^{\rm exact}(Born)$
0.0001
0.001
0.01
0.1
1
x

Fig.7a

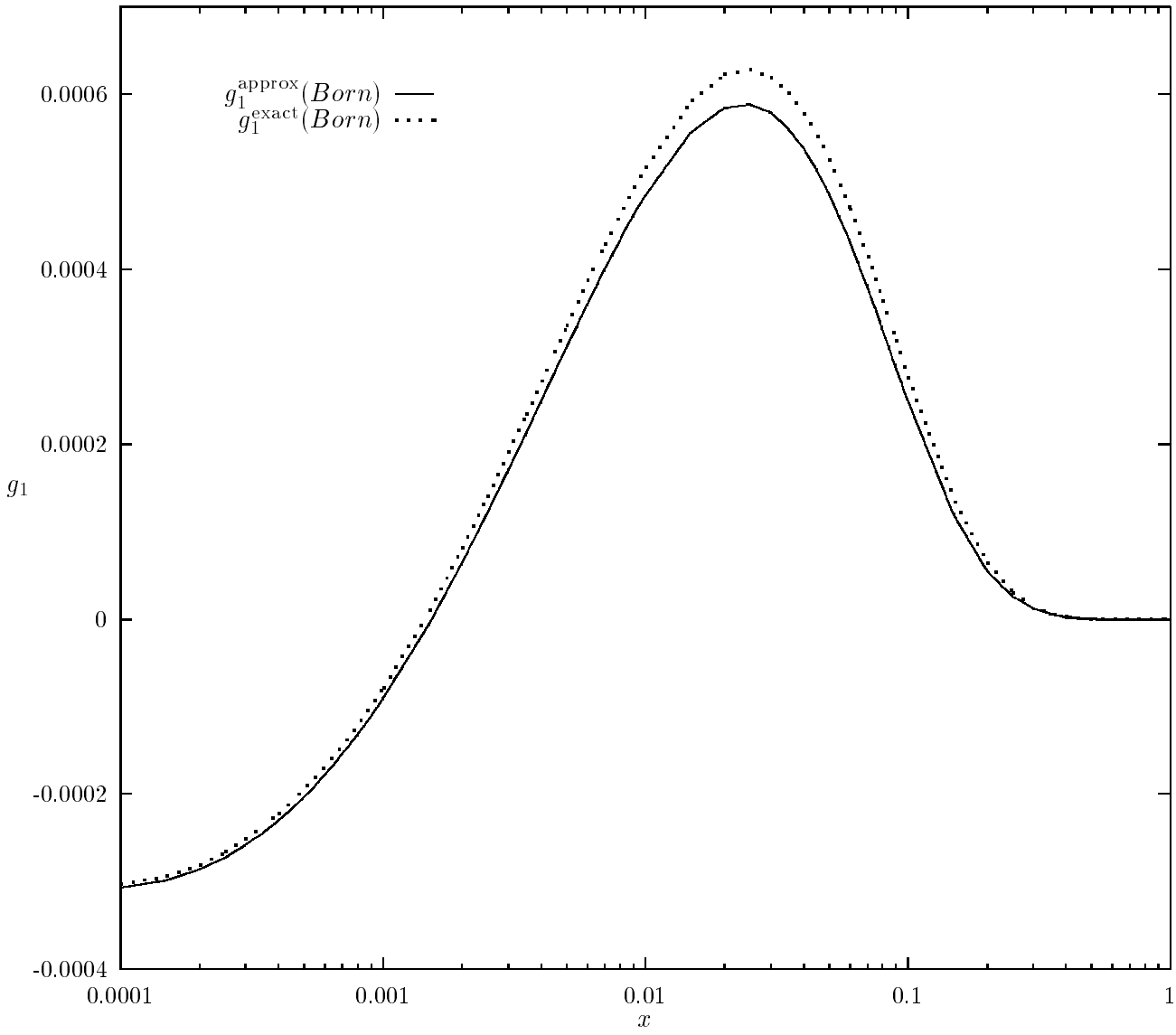
$g_1^{\rm approx}(Born)$
$g_1^{\rm exact}(Born)$
0.0006
0.0004
0.0002
0
-0.0002
-0.0004
g_1
0.0001
0.001
0.01
0.1
1
x

Fig.7b

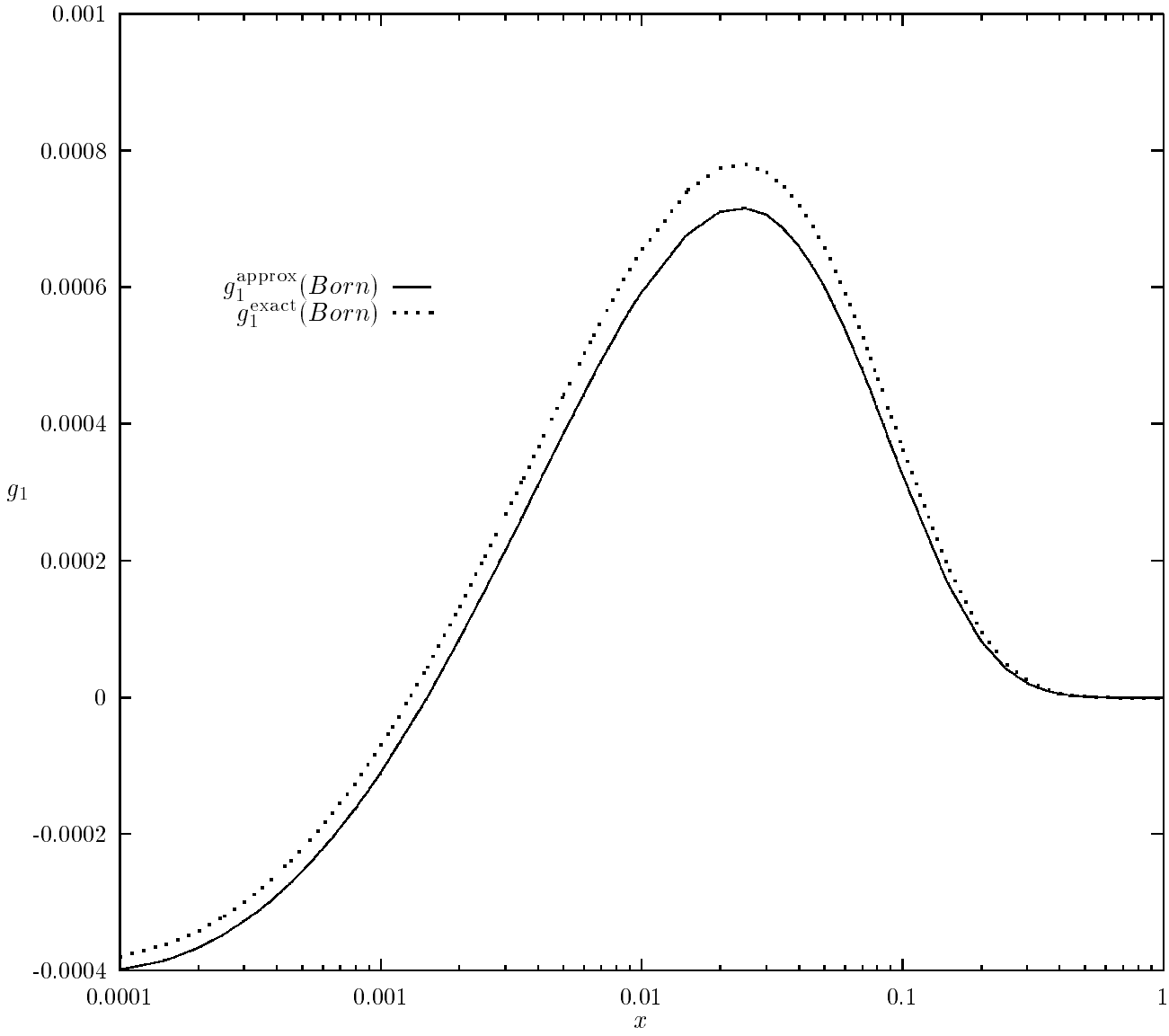
0.001
0.0008
0.0006
0.0004
0.0002
0
-0.0002
-0.0004
g_1
$g_1^{\rm approx}(Born)$
$g_1^{\rm exact}(Born)$
0.0001
0.001
0.01
0.1
1
x

Fig.7c

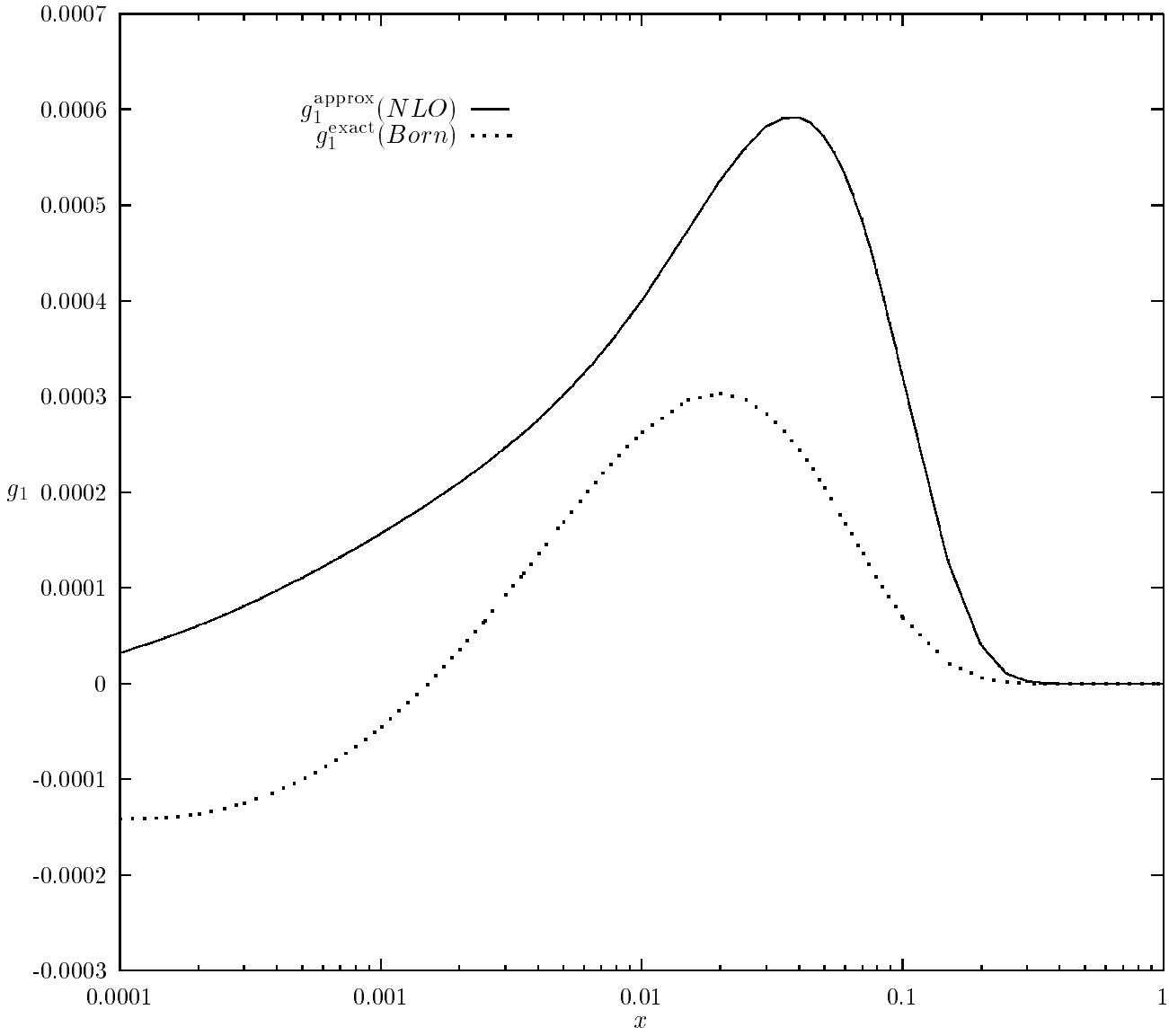
$g_1^{\rm approx}(NLO)$
$g_1^{\rm exact}(Born)$
0.0007
0.0006
0.0005
0.0004
0.0003
0.0002
0.0001
0
-0.0001
-0.0002
-0.0003
g_1
0.0001
0.001
0.01
0.1
1
x

Fig.8a

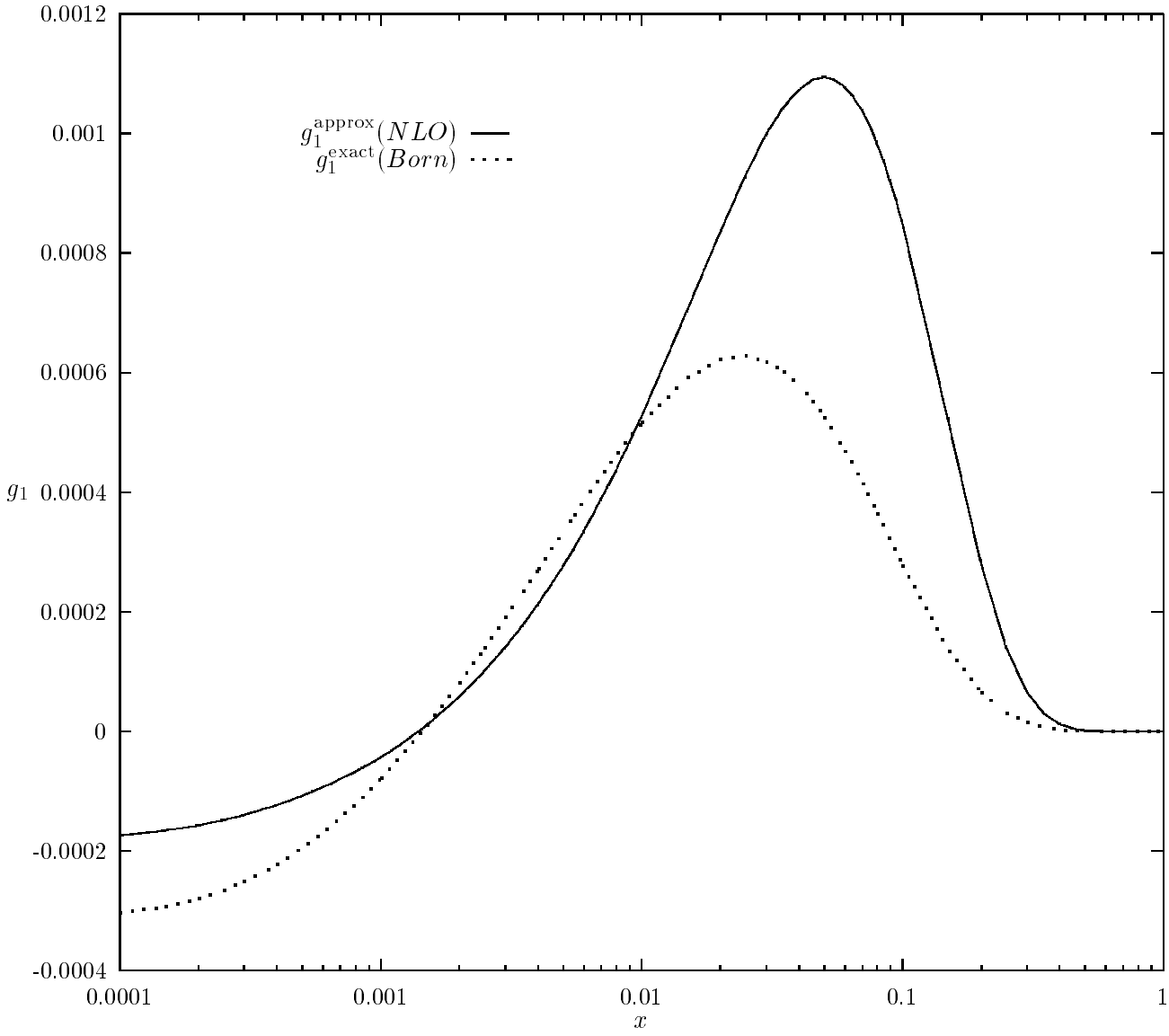
0.0012
0.001
0.0008
0.0006
0.0004
0.0002
0
-0.0002
-0.0004
g_1
$g_1^{\rm approx}(NLO)$
$g_1^{\rm exact}(Born)$
0.0001
0.001
0.01
0.1
1
x

Fig.8b

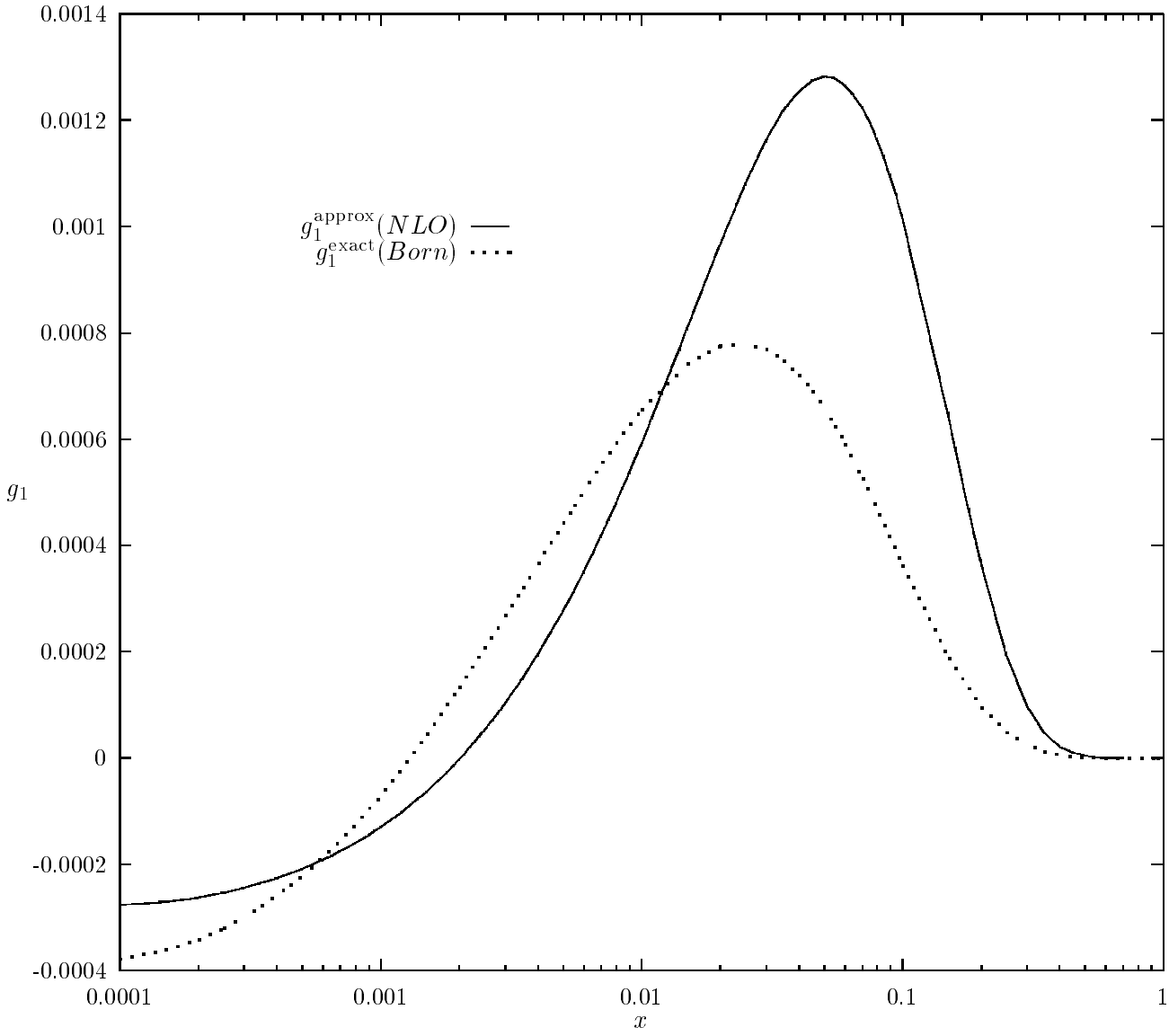
0.0014
0.0012
0.001
0.0008
0.0006
0.0004
0.0002
0
-0.0002
-0.0004
g_1
$g_1^{\rm approx}(NLO)$
$g_1^{\rm exact}(Born)$
0.0001
0.001
0.01
0.1
1
x

Fig.8c

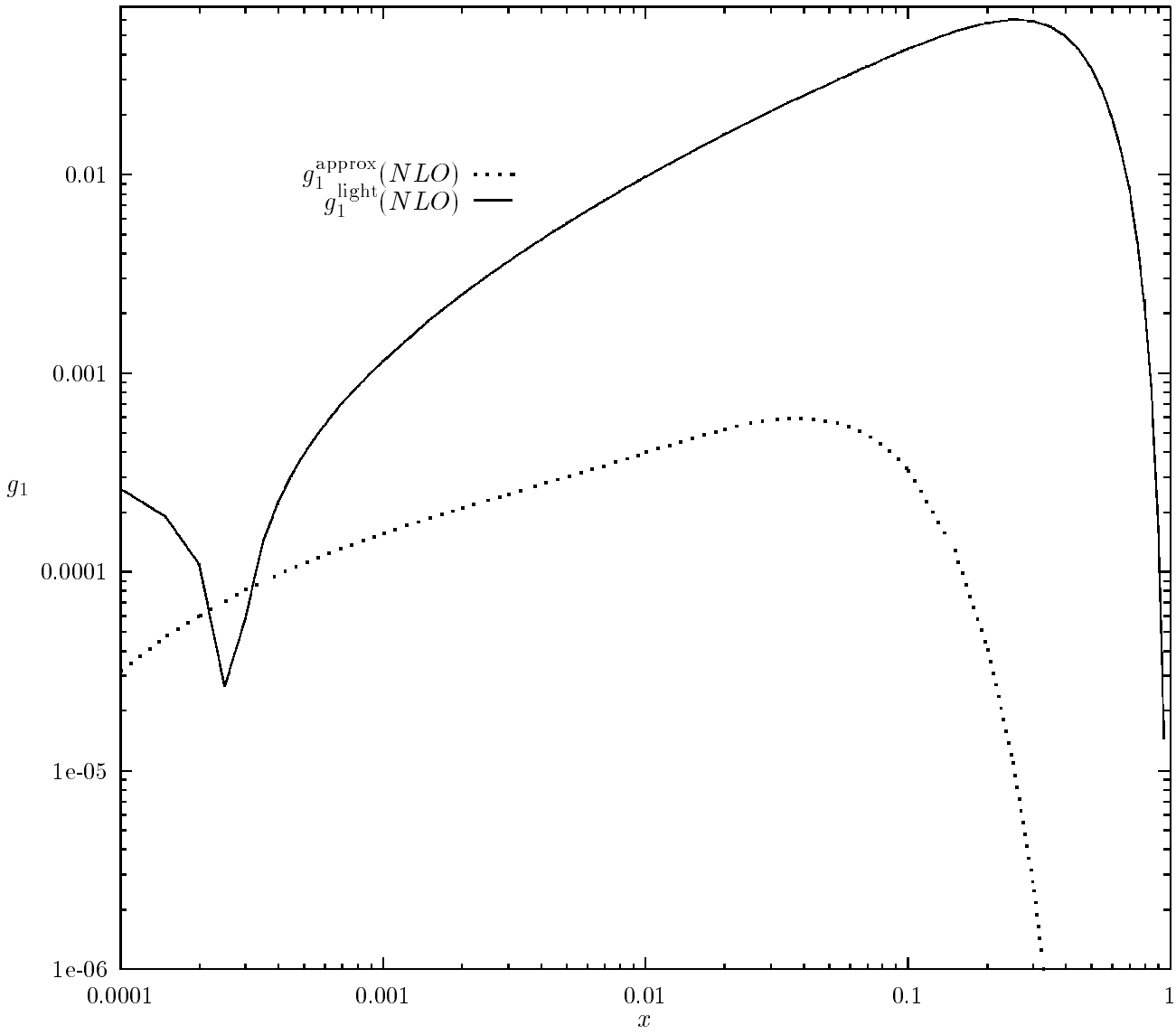
$g_1^{\rm approx}(NLO)$
$g_1^{\rm light}(NLO)$
0.01
0.001
0.0001
1e-05
1e-06
g_1
0.0001
0.001
0.01
0.1
1
x

Fig.9a

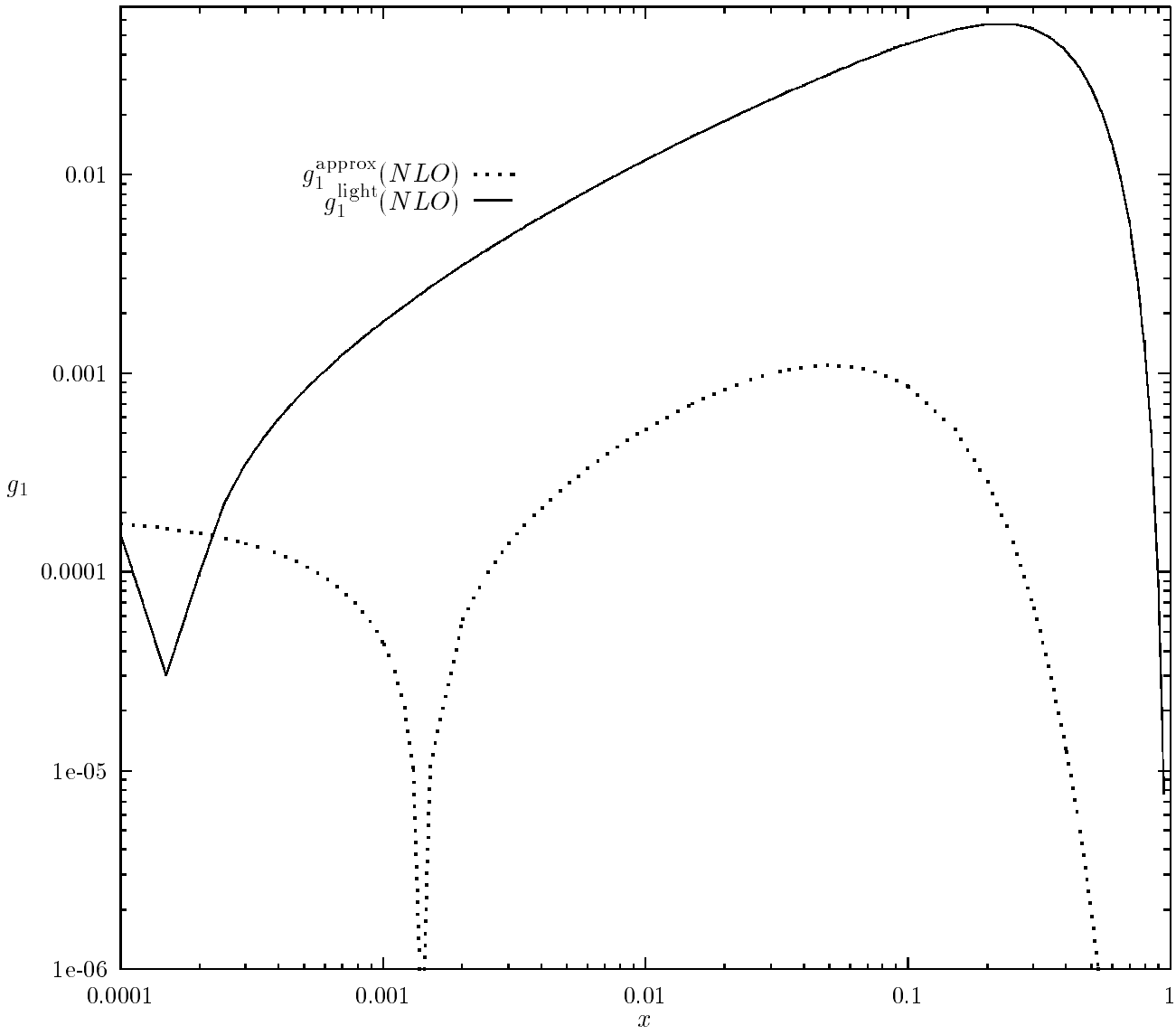
$g_1^{\rm approx}(NLO)$
$g_1^{\rm light}(NLO)$
0.01
0.001
0.0001
1e-05
1e-06
g_1
0.0001
0.001
0.01
0.1
1
x

Fig.9b

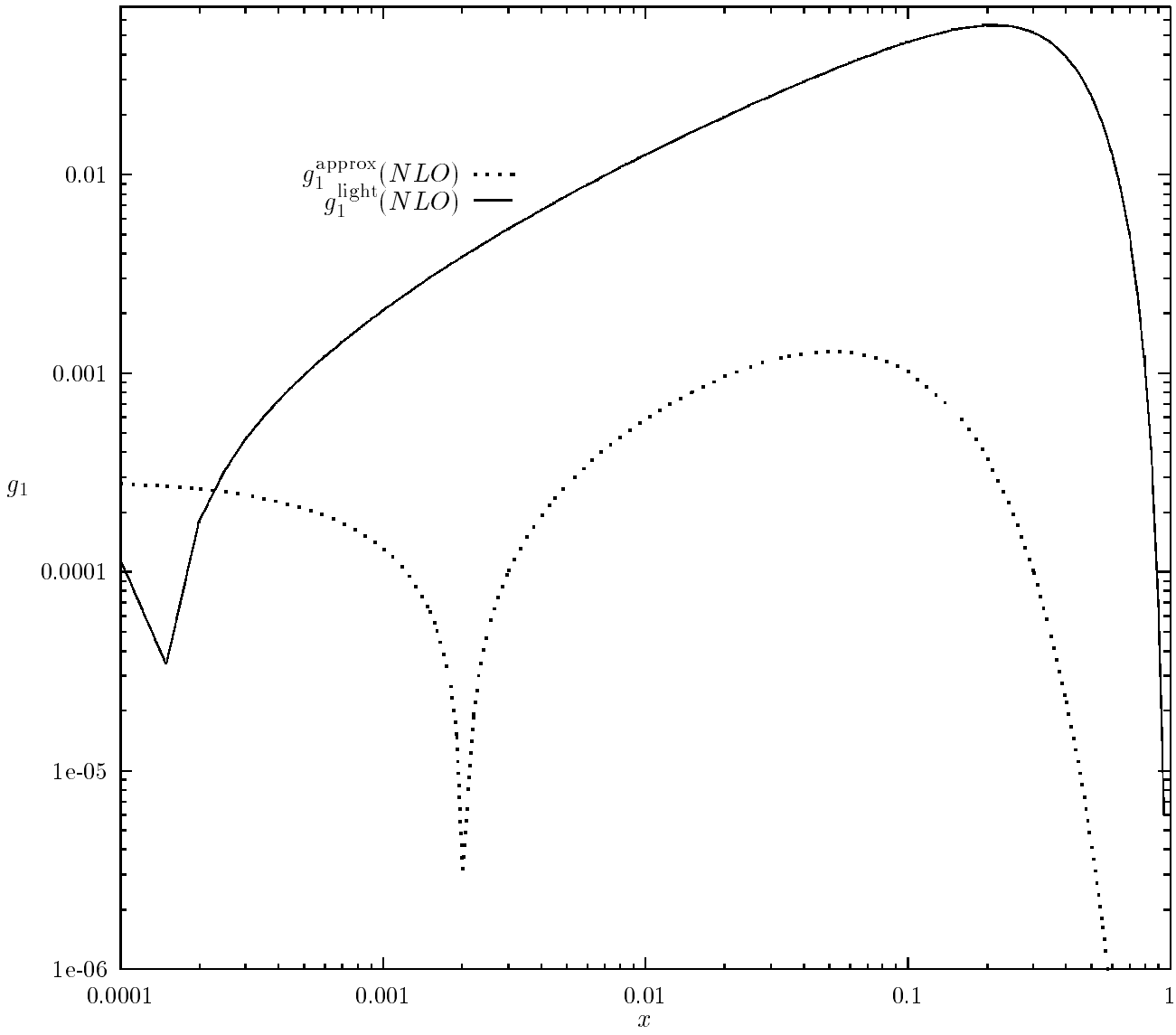
$g_1^{\rm approx}(NLO)$
$g_1^{\rm light}(NLO)$
0.01
0.001
0.0001
1e-05
1e-06
g_1
0.0001
0.001
0.01
0.1
1
x

Fig.9c